FINAL REPORT

Calibration of an Ion Mobility Spectrometer

28 May 1968 - 30 September 1969

Contract No.: NAS 5-11131

AVSD -127-70-RR

Prepared by

AVCO CORPORATION
Applied Technology Division
Lowell, Massachusetts 01851

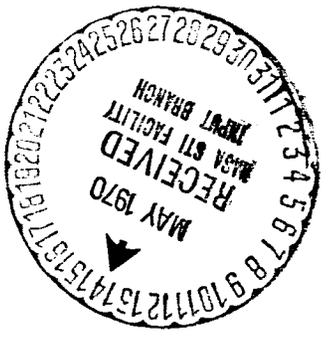

for

GODDARD SPACE FLIGHT CENTER
Greenbelt, Maryland

FINAL REPORT

Calibration of an Ion Mobility Spectrometer

28 May 1968 - 30 September 1969

Contract No.: NAS 5-11131
AVSD -127-70-RR

GODDARD SPACE FLIGHT CENTER

Contracting Officer: R. D. Phillips
Technical Monitor: A. C. Aikin 615

Prepared by

AVCO CORPORATION
Applied Technology Division
Lowell, Massachusetts 01851

Project Manager: W. T. Spencer

for

GODDARD SPACE FLIGHT CENTER
Greenbelt, Maryland

ABSTRACT

The objective of this program was to demonstrate that a correlation is possible between ion mobility spectra and ion mass spectra. The experimental study was conducted in the Avco low-pressure wind tunnel at simulated altitudes between 25 and 60 km. Subsonic air flow velocities were obtained by bleeding gas through the wind tunnel into an evacuated ballast tank. The mobility of ions generated by either a corona discharge or a radioactive source were measured with a cylindrical Gerdien Chamber. A quadrupole mass spectrometer mounted within a differentially pumped chamber was used to measure the mass spectra. Ions entered the quadrupole through a small (0.020 inch diameter) aperture.

Mobility and mass spectra have been recorded; however, a confident interpretation of the mass spectra is prevented because of uncertainties in the behavior of ions in the region of the aperture. Further examination of this question will, it is believed, result in the correlation between mass and mobility which is desired.

ACKNOWLEDGMENTS

The author wishes to acknowledge the assistance of two individuals not employed by Avco. Mr. S. Coroniti not only initiated the program, but also as an informal consultant contributed to its continuation. The initial measurements of mass spectra were made possible through the generosity of Dr. R. Narcissi who loaned a quadrupole mass spectrometer to Avco for our research. Finally, the support from Goddard Space Flight Center and Dr. A. C. Aikin is gratefully acknowledged.

TABLE OF CONTENTS

LIST OF FIGURES

LIST OF FIGURES (Cont'd)

1. INTRODUCTION

A program has been completed in which laboratory measurements with an ion mobility spectrometer have been compared with mass spectral measurements. As an introduction some remarks on ion mobility will be made.

If an electric field, E, is applied across any volume of slightly ionized gas, the negative and positive ions will be accelerated to the positive and negative electrodes, respectively. However, in their journey to the electrodes, the ions will experience many collisions with the neutral molecules of the gas. The path of each individual ion will be made up of a series of short runs, each terminating in a collision in which the accumulated energy of the ion is partially or totally lost. The ion, therefore, does not move with a uniform acceleration but rather drifts toward the electrode with an average velocity, v, which is given by the equation:

$$v = 1/2 \ \frac{E\,e\,T}{m} \tag{1}$$

where

E is the electric field strength
e is the charge of the ion
m is the mass of the ion
T is the time between collisions.

The quantity

$$k = 1/2 \ \frac{e\,T}{m} \tag{2}$$

is defined as the mobility of the ion. Hence, Equation (1) can be written

$$v = k\,E \tag{3}$$

or

$$k = \frac{v}{E} \tag{4}$$

The difinition of mobility, k, is the velocity of the ion divided by the electric field strength in which it is moving.

The value, k, as seen from Equation (2), involves the time interval, T, between collisions. T is dependent on the thermal velocities of the ions and on the mean free path.

The mobility of an ion is inversely proportional to the gas density ρ :

$$k_1 = \frac{\rho_2}{\rho_1} \quad k_2 \tag{5}$$

where the indices 1 and 2 correspond to different height levels.

Since the air density decreases exponentially with height, it is evident from equation (5) that the mobility increases correspondingly. Consequently at any given temperature and pressure, a measurement of mobility, k, is also a measurement of the mass m of the ion or ion cluster.

This simplified derivation is used only to indicate the basic relation between k and m. A more detailed discussion of the theory is given in Avco Report RAD-TR-65-25 (pp. 8-20) (Dolezalek and Oster, 1965).

Somewhere in the region of 30 to 80 km, the electrical composition of the atmosphere changes from an ion to an ion-electron regime. We shall refer to it as the "transition region." Until the last five years or so, its lower part was totally neglected. The atmospheric electricity physicists were interested in the electrical properties of the atmosphere below 30 km; the ionospheric physicists devoted their attention exclusively to the atmosphere bounded by 65 to 500 km. As a consequence, the nature and number density of the atmosphere is much better known below 30 and above 80 km than within the transition region.

Until recently, the molecular-ion, atomic-ion, and electron constituents of the transition region were derived, in the main, from theoretical considerations. One serious difficulty with this approach is the total lack of precise knowledge of the rate coefficients, which are very important factors in the photochemical reaction equations.

What is needed in order to compute the rate coefficients are accurate measurements of densities and sizes of the ion species within this altitude of 30 to 80 km. The availability of such carriers as high flying balloons and rockets gave scientists, for the first time, the means to transport scientific instruments of all types of these altitudes. Avco has developed an instrument which will measure the mobility directly -- from which size and species can be derived -- and which will count the number of positive and negative ions as well as electrons within this transition region. In developing this instrument, it was necessary to build a low-pressure wind tunnel facility in order to calibrate it. To Avco's knowledge, it is the only facility of this kind in existence.

We have just stated that an ion mobility spectrometer can be used to measure size, density and species of ions in the transition region. This is true in principle; however, it is not certain, a priori, that one can interpret the mobility spectrum measured and deduce from it the desired data. It was

the objective of this program to show by laboratory measurements of the mobility and mass that this correlation could be made.

The first quotation of a method for the measurement of mobility is found in Rutherford's paper of 1899. Zeleny and Lenard, both in 1900, and Kähler in 1903 applied about the same principle, before Gerdien turned it (1905) into the most common tool for the measurement of the polar electric conductivities in the atmosphere. Since then, the condenser as used here -- mostly a cylindrical one -- is often referred to as the "Gerdien condenser," "Gerdien chamber," "Gerdien counter", or simply the "Gerdien".

The Avco Gerdien chamber will be discussed in detail in a later section. Basically ions are carried through the chamber in a wind of neutral molecules. Because of the transverse electric field the ions travel to collectors with a drift velocity which can be calculated from the chamber geometry and which depends upon the strength of the electric field. The mobility can be obtained from equation (4).

Implementation of the program was through the use of the Avco low-pressure wind tunnel. Measurements of both mobility and mass were made in this environment and attempts at correlation can be made.

To facilitate planning and supervision of the program, a series of six tasks were devised to cover its various aspects:

1000	Mass Spectrometer
2000	Wind Tunnel
3000	Ion Mobility Spectrometer (IMS)
4000	Calibration Tests of Avco IMS
5000	Calibration Tests of GSFC IMS
6000	Reports

Where required, subtasks have been identified. In the second section of this report, each of the tasks will be examined in detail. In summary, the first three tasks were devoted to the preparation of the three major systems to be used in the program. In Task 4000, the Avco Ion Mobility Spectrometer was tested and correlations were attempted with mass spectrometric observations. A GSFC-supplied ion mobility spectrometer was similarly studied in Task 5000. Task 6000, Reports, is self explanatory.

II. PROGRAM TASKS

A. Mass Spectrometer (Task 1000)

As outlined in the introduction, the objective of the program was to compare the results of ion mobility measurements with experimental determinations of ionic mass distributions.

In general, mass spectrographs consist of three elements: a "source" in which the gas or vapor investigated is ionized; an "analyzer" in which particles of equal charge to mass ratio are focussed to a common location; and finally, a "read-out" in which the results of the mass analysis are translated into an electrical or photographic signal. When, as for the case of interest, only ions need to be analyzed, the design of the source is eliminated since the charged particles already exist. There is however the new problem of focussing the ions into the entrance aperture of the mass spectrometer.

The choice of the most suitable spectrograph for a given application depends on a variety of factors. For the case in point, the most important considerations are of a practical nature; namely, ease of operation and read-out, availability, and finally, future course of the investigation. These factors limited our choice of possible instruments to two types: quadrupole and small-sized magnetic-sector mass analyzer.

Both have electronic read-out and capability of rapid scan acros the mass range. The quadrupole has the added advantage that similar devices have been used in rocket and satellite research and that data obtained on this type of instrument may be of direct use for the analysis of results from an on-flight experiment.

Dr. R. Narcissi of AFCRL has generously allowed us to borrow for these studies a quadrupole mass spectrometer of the type he has used in several rocket flights. This instrument was used in our initial measurements. A commercial instrument was obtained subsequently. Both mass spectrometers will be described in a later section.

The operating pressure in a mass spectrometer is limited to, at most, a fraction of a micron because of collisions between the ions and the residual gas. If species of a low concentration are to be observed, the maximum pressure must be even lower, perhaps 10^{-5} torr. Thus, we must provide some means of reducing the pressure from the value of interest (in the wind tunnel) to a reasonably low value.

In some systems, this can be done by providing a leak between the high pressure region and the mass spectrometer. However, if ions present in a high-pressure region are to be analyzed, the gas containing the ions must be able to reach the analyzing region of the spectrometer without making many collisions with walls of the apparatus. A small leak cannot be used. Rather, differential pumping, with a direct line-of-sight path between the high pressure region and the analyzing region, must be used. Part of Task 1000 was the design and assembly of a suitable differential pumping system. The major position of the task was devoted to placing the instruments in operation and experimentation with various ion optical configurations. This effort will also be treated in a later section.

B. Wind Tunnel (Task 2000)

As part of earlier development efforts on the Avco Ion Mobility Spectrometer, a wind tunnel facility was built in which the air velocity and pressure the instrument experiences during an actual flight (up to about 80 km) can be simulated. The wind tunnel is 8 inches in diameter and approximately 15 feet long. It is connected through various valves to a 10,000 cubic foot ballast tank at the downstream end. Specific gases can be admitted at the up-stream end through leak valves. By properly adjusting the leak valves and the exhaust valves, the velocity and pressure in the tunnel can be set over a wide range. The duration of a test depends on the leak rate used; for high leak rates, the test must end when the ballast tank pressure rises and alters the wind tunnel parameters. For low leak rates, the central vacuum system has sufficient capacity to maintain the ballast pressure.

The size of the mass spectrometer and its vacuum system required the wind tunnel to be modified to receive it. To avoid the problems of a "ship-in-a-bottle" design, an enlarged segment for the tunnel was used. A side entry port allowed easy mounting and alignment of the mass spectrometer.

As with any vacuum system which has been idle for an extended period, an effort of cleaning and reactivation of the tunnel was required. These activities were part of Task 2000.

In past studies of the characteristics of the ion mobility spectrometer, a radio-active source was used to produce the required ion. While this source was extremely stable, the ion density produced was very small leading to detected ion currents which were difficult to measure. To avoid this handicap, a glow discharge was chosen as an alternate ion source for the current program. Tests of this source have been conducted as part of the wind tunnel task.

C. Ion Mobility Spectrometer (Task 3000)

The principles of operation of the ion mobility spectrometer (IMS) have been outlined in the introduction. Complete details will appear later.

Task 3000 was to put the Avco IMS in operation and assure that the associated electronics were operating properly. Upon completion of this task and tasks 1000 and 2000, the three systems of the program were operational and the actual correlation experiments could begin.

D. Calibration Tests of the Avco IMS (Task 4000)

The task of calibration of the Avco IMS consisted of the measurement of mobilities and ion mass concentration in the wind tunnel. These measurements were made with air and pure nitrogen.

E. Calibration Tests of the GSFC IMS (Taks 5000)

Procedures similar to the correlation studies made with the Avco IMS were attempted using a GSFC furnished instrument. Because of schedules only one effort of two days was possible with the GSFC device. A section of this report is devoted to those measurements.

III. SUPPORT FACILITIES

A. Wind Tunnel

The Avco low-pressure wind tunnel is one of two support facilities necessary to the implementation of this research program. The wind tunnel is constructed from 8 inch diameter pipe sections interconnected by flanges and connected to a 10,000 cubic foot ballast tank through a network of valves at the downstream end. Specific gases can be admitted at the upstream end through leak valves. The facility is shown schematically in Figures 1 and 2.

Air flow (or wind) is obtained and controlled in the tunnel by adjusting an upstream inlet leak valve and the downstream exit valves. The pressure and velocity in the tunnel are thus determined by these valve settings and the ballast tank pressure. The pumping system for the ballast tank is shown in Figure 3.

During the development of the wind tunnel facility, tests were made to determine the pressures and velocities attainable. In Figure 4 each point represents a velocity measurement at a particular static pressure.

It can be seen that pressure and velocity can be regulated independently. For example, at a static pressure of 500 millitorr (corresponding to a height of 55 km), a number of different wind speeds between 0.1 and 2 Mach have been simulated. Even much slower wind speeds, than those given in this figure, can be obtained at this static pressure. However, the accuracy of the velocity measurement becomes more and more inaccurate the lower the velocity of the streaming air.

The maximum speed which can be obtained can be determined from the pumping speed of the pumps. The lines in Figure 4 give the theoretical obtainable values. As can be seen at pressures above 10 torr (corresponding to heights below 30 km), the obtainable velocity is less than 0.3 Mach.

The static pressure in the wind tunnel is measured with an alphatron vacuum gauge. The dynamic range of this instrument is from atmospheric pressure to 10^{-4} torr. Flow velocities are obtained from pressure differences in a pitot tube. A Baratron differential pressure gauge is used to sense the difference between the impact pressure and the static pressure. The Baratron can detect quantities as small as 3×10^{-5} torr. The flow velocity is a function of the ratio of the impact pressure to the static pressure, P_t/P_s:

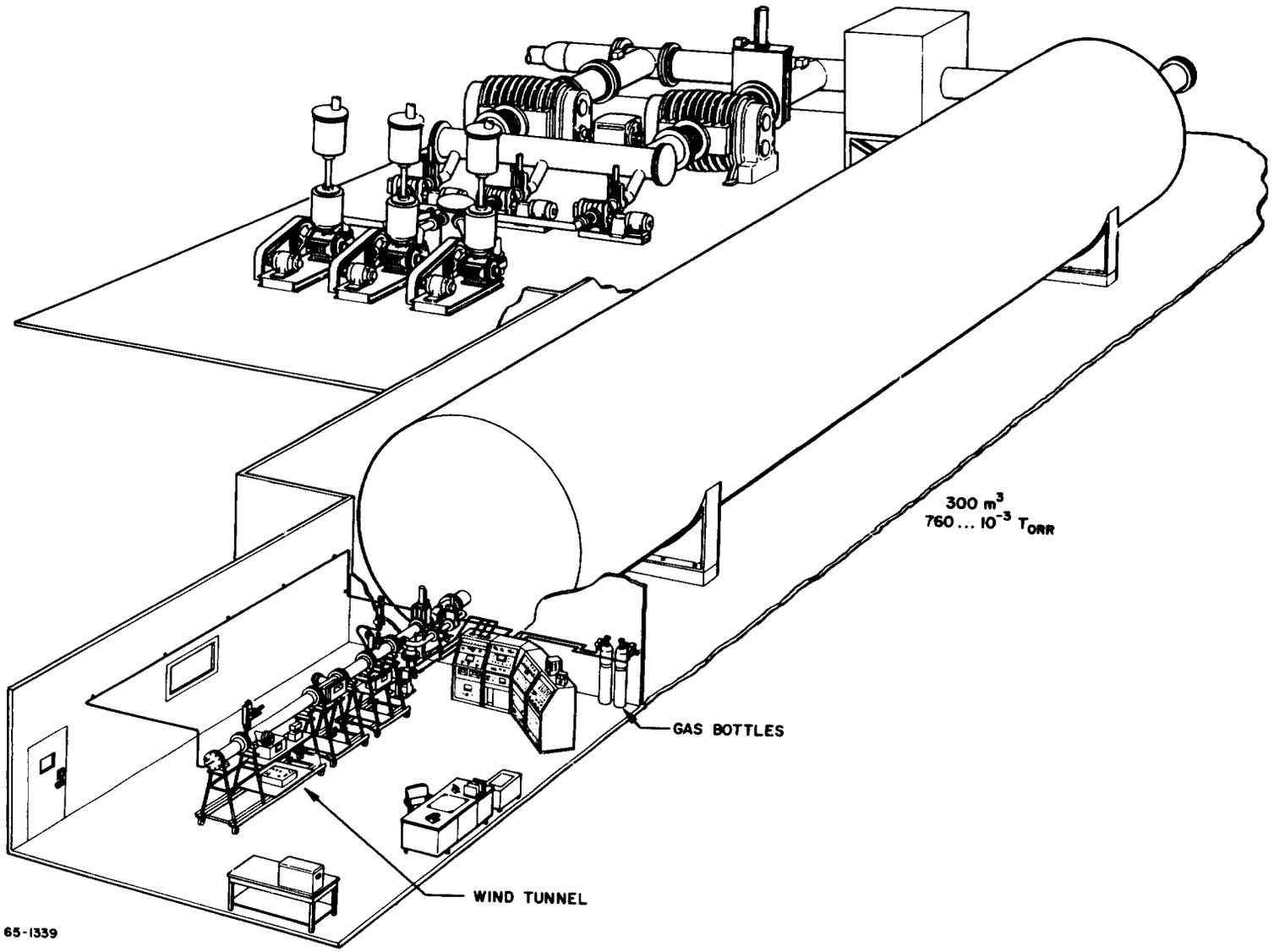

Figure 1 LOW-PRESSURE WIND TUNNEL

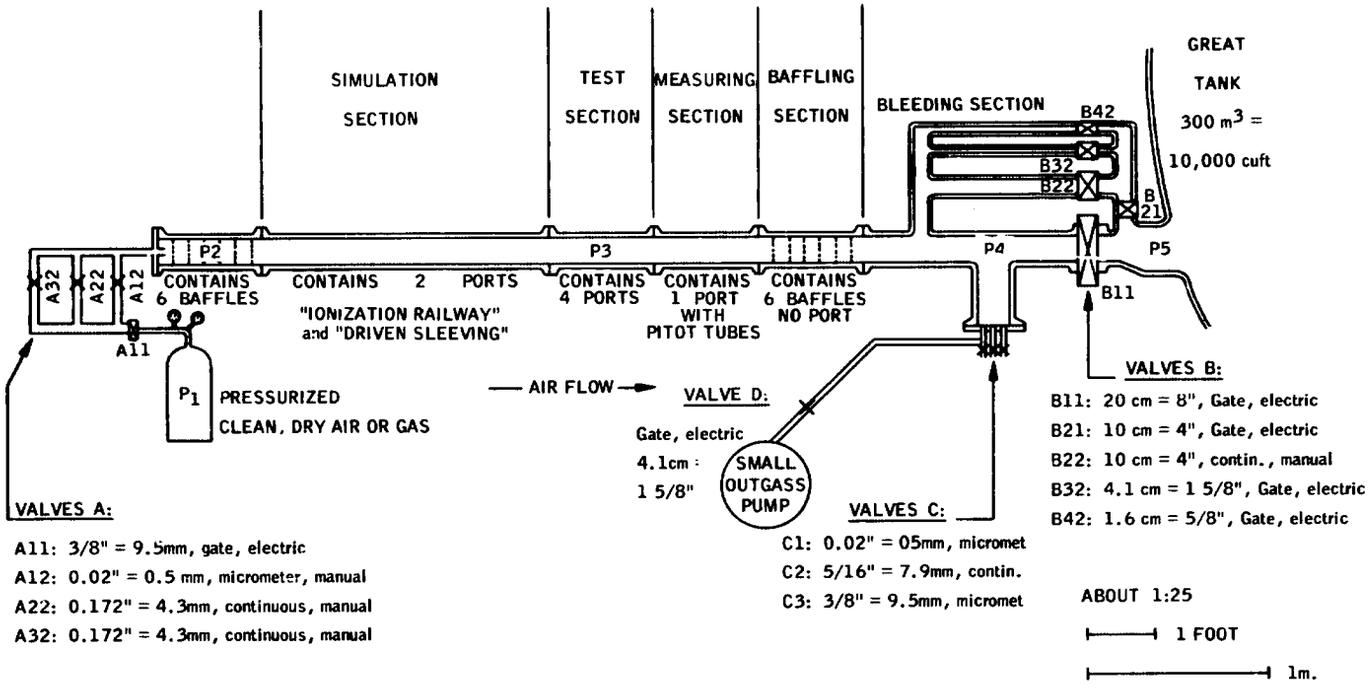

64-11968

Figure 2 CROSS SECTION OF WIND TUNNEL

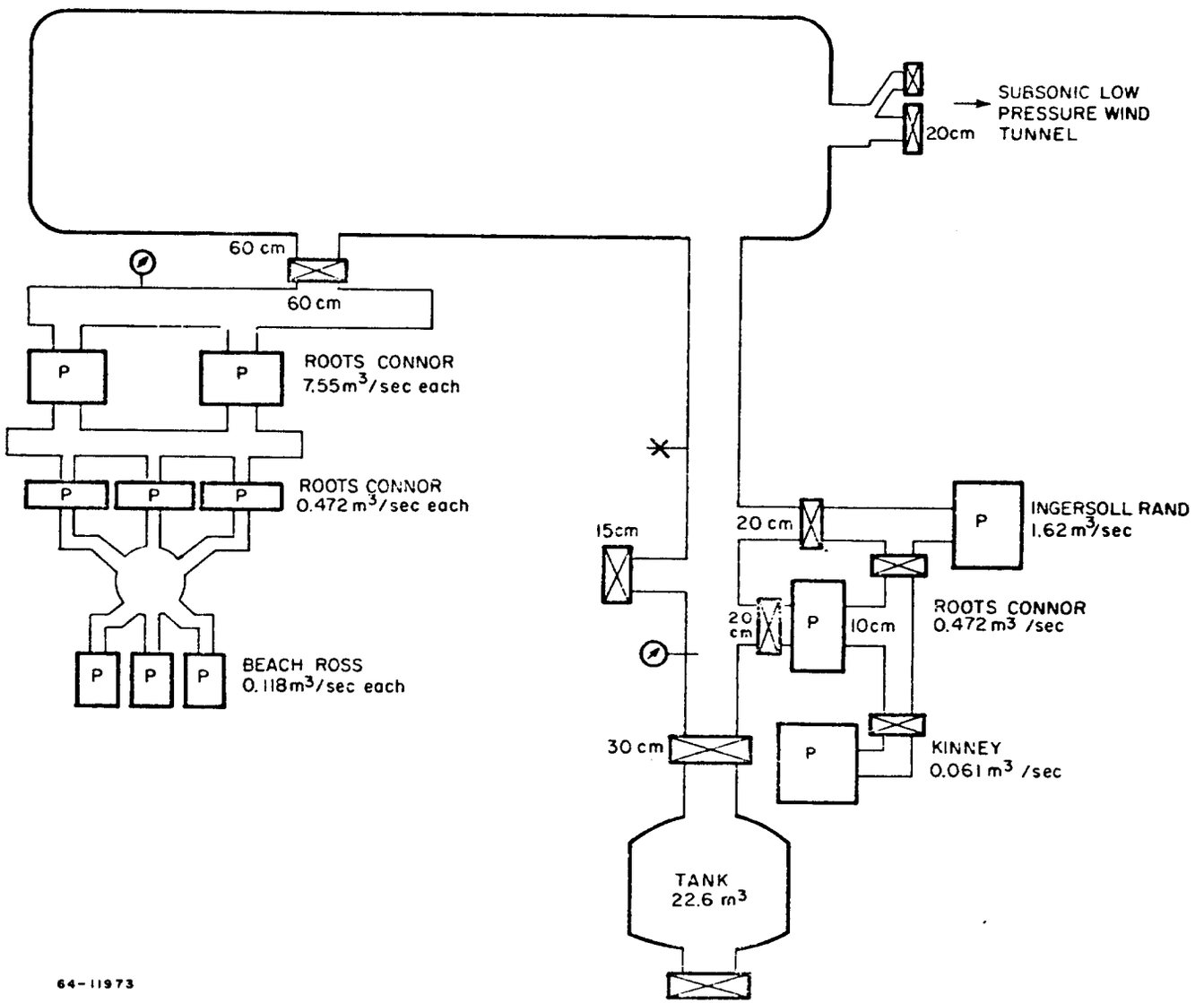

Figure 3 OVERALL SYSTEM OF THE SUBSONIC LOW-PRESSURE WIND TUNNEL

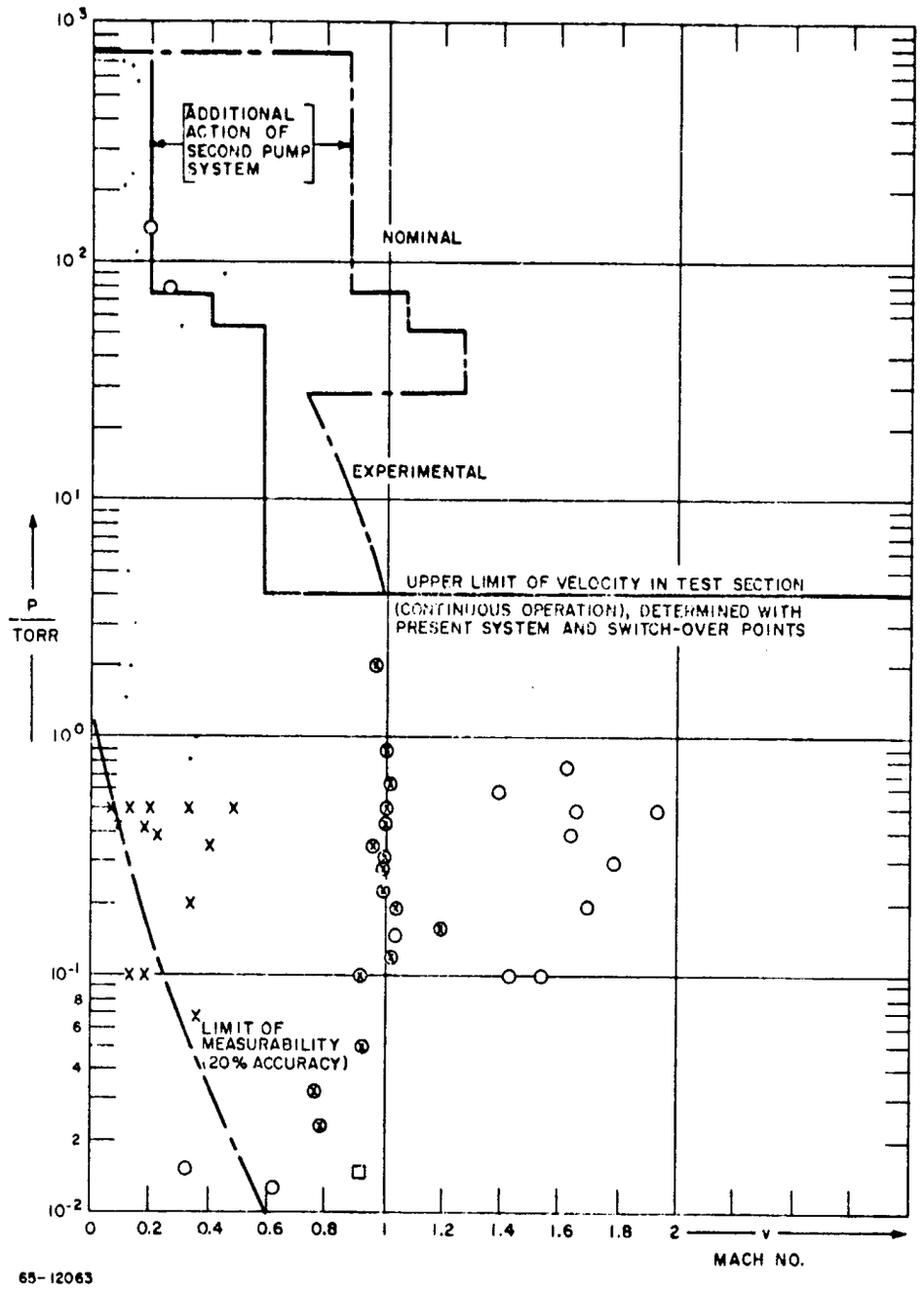

Figure 4 PV-DIAGRAM OF LOW PRESSURE WIND TUNNEL FOR CONTINUOUS OPERATION

(Points: Experimental values obtained under different experimental conditions)

$$\frac{P_t}{P_s} = \left(1 + \frac{\gamma - 1}{2} M^2\right)^{\frac{\gamma}{\gamma - 1}} \qquad (6)$$

For subsonic flow.

where

P_t = the total or impact pressure

P_s = the static pressure

M = the Mach number or ratio v/c with c = speed of sound

γ = the ratio of specific heats: c_p/c_v
(for air at 20°C, $\gamma = 1.4$).

Substituting the numerical value for γ and solving for M we obtain

$$M = \sqrt{5\left[\left(\frac{P_t}{P_s}\right)^{2/7} - 1\right]} \qquad (7)$$

Other equations can be derived for supersonic flow.

A source of ionization was generally located near the upstream end of the wind tunnel. This gave the plasma an opportunity to approach an equilibrium state before reaching the mobility spectrometer or the mass spectrometer. It was found that two kinds of sources were necessary over the pressure range of interest. At higher pressures, above about 3 torr, a radioactive source of polonium -210 emitted sufficient ionizing radiation to produce measurable ion densities. Of course this was a very stable source. At pressures below one torr the ionization cross section became too small for this source to function. Over the range from a few microns to a few torr a corona discharge was found to produce an abundant supply of ions. A wire probe projecting into the wind tunnel was operated at a negative potential between 0.5 and 2.5 KV. The air flow would carry the ions downstream away from the visible plasma sheath which surrounded the probe.

B. Mass Spectrometer Vacuum System

It has been pointed out in Section II that the pressure requirements of a mass spectrometer (below 10^{-4} torr) necessitated the use of a differentially pumped vacuum system. Initial calculations suggested three stages of pumping with three chambers separated by apertures.

A three chamber system was assembled and tested with the AFCRL quadrupole mass spectrometer. The vacuum characteristics were to an order of magnitude as predicted. However, it was found that with three consecutive apertures the loss of ions was excessive. No mass spectra could be seen.

It had been assumed, when the apparatus was designed, that almost all ions entering the first orifice would pass through the other two and be detected by the spectrometer. Because of the results cited above, the ion beam current was recalculated assuming a cosine distribution at the first pinhole and 100 percent transmission at the third. In this calculation, data from Gerdien chamber measurements were used. If the total ion current entering the Gerdien is 10^{-10} A, then from a ratio of areas, the current entering the first pinhole is 10^{-14} A and that passing through the second and third to enter the quadrupole is 10^{-20} A. Since the sensitivity of the AFCRL instrument was about 10^{-15} A, we should not be surprised by our negative results if the assumptions used above are correct.

To circumvent this loss of six orders of magnitude in current, it was decided that the first two differentially pumped chambers would be removed, leaving a single .020 inch diameter orifice. This meant that with the existing diffusion pump and liquid nitrogen baffle, the upper limit of wind tunnel pressure would be adversely affected. This upper limit turned out to be 100 microns (0.1 torr).

Because of the schedule requirements at AFCRL it was necessary to return the borrowed quadrupole mass spectrometer in mid-contract. The replacement instrument, obtained from GSFC will be described in detail in a later section. Modifications to the mass spectrometer vacuum system were made to accommodate this change and to improve the pumping characteristics. A diagram of the final configuration will be found in Figure 5. The mass spectrometer was mounted in one arm of a standard Varian 4-inch TEE; the opposite flange carried the pinhole plate. At the side arm of the TEE, connection was made through the wind tunnel wall to a 4-inch liquid nitrogen cooled chevron baffle and a 4-inch oil diffusion pump. A Welch Duoseal model 1397 mechanical pump (17.7 cfm) provided the fore vacuum. With this improved configuration the upper limit on wind tunnel static pressure turned out to be about 800 microns (0.8 torr).

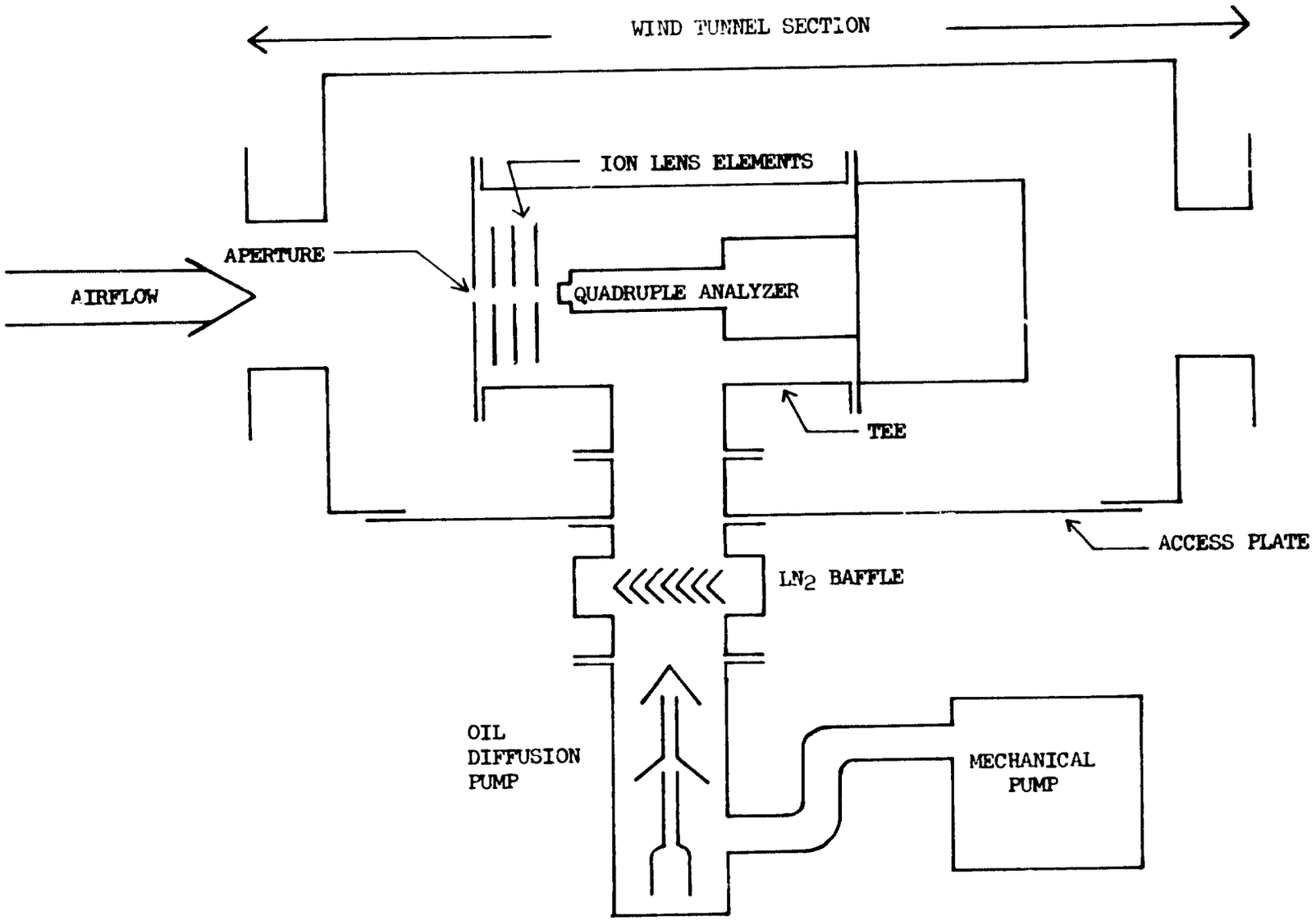

FIGURE 5. MASS SPECTROMETER VACUUM SYSTEM

IV. GERDIEN CHAMBER

A. The DC Ion Mobility Spectrometer

The concept of ion mobility was presented in the Introduction. In this section, we describe the DC mobility spectrometer, developed by Avco, which was used in this program.

Figure 6 illustrates the basic principle of the DC ion mobility spectrometer. We assume an airstream containing ions of three kinds characterized by three mobilities, k_A, k_B, and k_C. They enter a series of three plate condensers, A, B, and C. The length of each is w, and the plate separation is d. Air enters all the slits at the left of the chamber and flows parallel to the plates of the condenser at a velocity u which is uniform throughout a cross section. An electric filter allows ions to enter only through one small slit (ion gate), of width Δ y and at a vertical distance d from the negative plates of the condenser. Therefore, in the absence of any plate voltage, the ion velocity equals the velocity of the airflow within the chamber. When a DC voltage, V, is applied across the plates, an electric field, $E = \frac{V}{d}$, is produced.

Under the influence of this electric field, the ions move with velocity component $v = kE$ perpendicular to the plates. The positive ions are thus deflected toward the negative plates from their horizontal path. The trajectories of these ions within the chamber are given by the following equation (see Figure 6):

$$\frac{x}{y} = \frac{kE}{u} \tag{8}$$

It can easily be seen that all ions whose mobility is

$$k_A \leq \frac{d}{w} \quad \frac{u}{E} \tag{9}$$

will be collected on condenser plate A. Those ions whose mobility k_B is described by

$$\frac{d}{w} \quad \frac{u}{E} < k_B \leq \frac{d}{2w} \quad \frac{u}{E} \tag{10}$$

will be collected on condenser plate B. And finally, all ions whose mobility k_C is described by

$$\frac{d}{2w} \quad \frac{u}{E} < k_C \leq \frac{d}{3w} \quad \frac{u}{E} \tag{11}$$

will be collected on the last condenser plate.

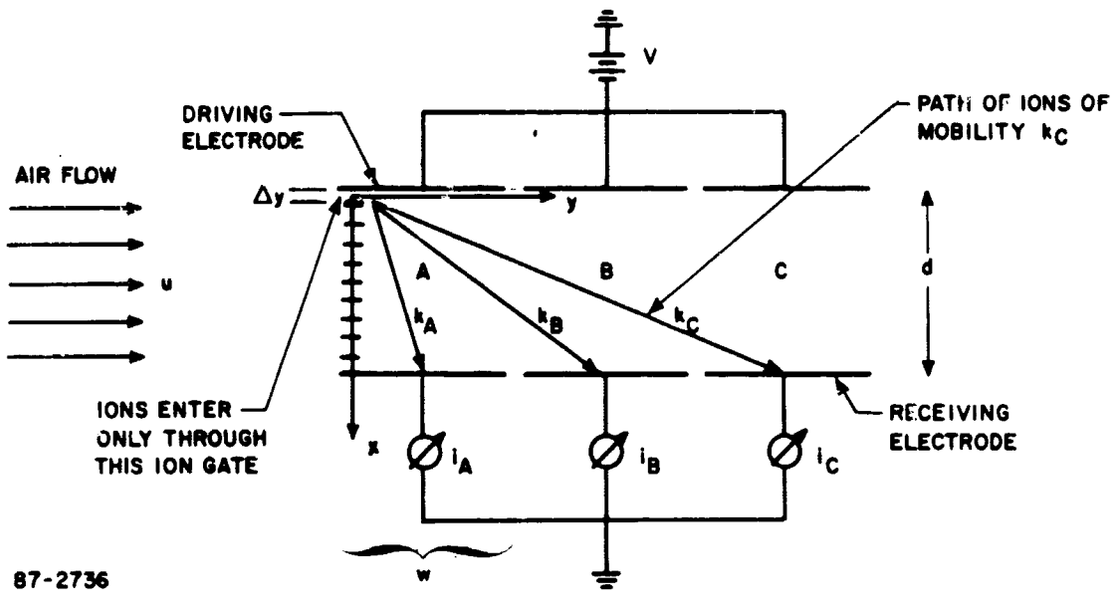

Figure 6 BASIC PRINCIPLE OF DC MOBILITY SPECTROMETER

The currents i_A, i_B, and i_C are a measure of the number of ions which impinge on collector plates A, B, and C, respectively, having mobilities in the three bands defined by the inequalities (9), (10), and (11).

If an alternating voltage were applied between the condenser plates the resulting instrument would be termed an AC ion mobility spectrometer. Its operation is described elsewhere (Dolezalek and Oster, 1965).

B. Mobility Measurement Technique

A laboratory model of an ion mobility spectrometer had been built and tested in Avco's low pressure wind tunnel. A cross section of this instrument is shown in Figure 7, and a picture of it in Figure 8. The measurements of mobility made for this contract were obtained with the spectrometer shown in Figure 8 operating in the DC mode.

As shown in Figure 7, the Avco IMS has three sets of eight concentric rings at the upstream end and one such set at the downstream end, a series of driving electrodes along a central rod, and 16 collector rings concentric with the central rod. Several modifications to what might be called normal operation of the IMS were made for the measurements reported below. The most upstream set of rings was removed. The rings of the remaining two upstream sets were interconnected so that electrically they formed a single set (i.e., 10 to 20, 11 to 21, etc.). No connection was made to the downstream set. All driving electrodes were wired together and all collectors but one were connected directly to ground. The remaining collector was grounded through the vibrating reed electrometer used to measure the ion current.

Before making the actual mobility spectrum measurements, preliminary measurements were made to determine the optimum value of the fence voltage, V_F. The upstream rings were wired to form what is called a double solid fence; double because it is made with two sets of rings, solid because there is no gate, and fence because the voltage V_F is applied between alternate rings generating a strong local transverse field to prevent ions from entering the Gerdien Condenser proper. With $V_F = 0$, the driving voltage, V_D, was adjusted to produce a maximum ion current at one of the collectors (No. 42 was used). Then with V_D held constant, V_F was increased until the ion current was cut off.

Having determined the optimum value for V_F, the upstream rings were rewired to form a double fence with a gate. The arrangement is shown schematically in Figure 9. It can be seen that the transverse field between ring 16 and ring 17, for example, will sweep charged particles from the flowing air and allow only neutrals to continue. Between rings 11 and 12 and between 21 and 22 there is no field. Thus there is a gate in the fence

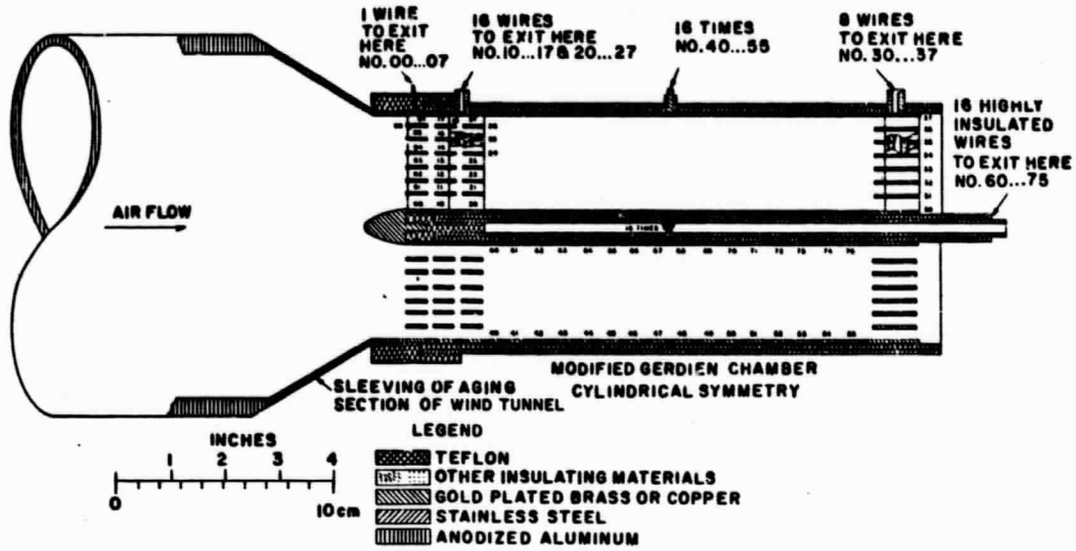

ELECTRODES AND RINGS (ALL GOLD PLATED):

FIRST SET OF RINGS, NO. 00...07	:	EQUALIZING RINGS, EXTERNAL (EDGE EFFECT CANCELLATION)
SECOND SET OF RINGS, NO. 10...17	:	ION FENCE WITH ION GATE
THIRD SET OF RINGS, NO. 20...27	:	EQUALIZING RINGS, INTERNAL, UPSTREAM (FIELD EQUALIZING)
FOURTH SET OF RINGS, NO. 30...37	:	EQUALIZING RINGS, INTERNAL, DOWNSTREAM (FIELD EQUALIZING)
OUTER ELECTRODES, NO. 40...55	,	USED AS RECEIVING ELECTRODES
INNER ELECTRODES, NO. 60...75	,	USED AS DRIVING ELECTRODES

EXAMPLE FOR ELECTRIC CONNECTIONS: IF THE ION GATE IS BETWEEN 13 AND 14, THE FOLLOWING RINGS WILL BE DIRECTLY CONNECTED TO EACH OTHER: 23-24-14-00-01-02-03-04-05-06-07-11-16 AND TO THE SLEEVING OF THE AGING SECTION OF WIND TUNNEL. ALSO 10-12-15-17 WILL BE INTERCONNECTED. THE FENCE VOLTAGE IS BETWEEN 10 AND 11. THE GATE VOLTAGE IS BETWEEN 13 AND 14.

THE RINGS ARE MOUNTED ON THREE TEAR SHAPED LEGS. ALL RINGS CAN BE TAKEN OUT AND REPLACED BY A SET OF THREE LEGS WITHOUT INTERMEDIATE RINGS (FULLY OPEN INTAKE AND OUTLET).

64-11972

Figure 7 AC ION MOBILITY SPECTROMETER (CROSS SECTION)

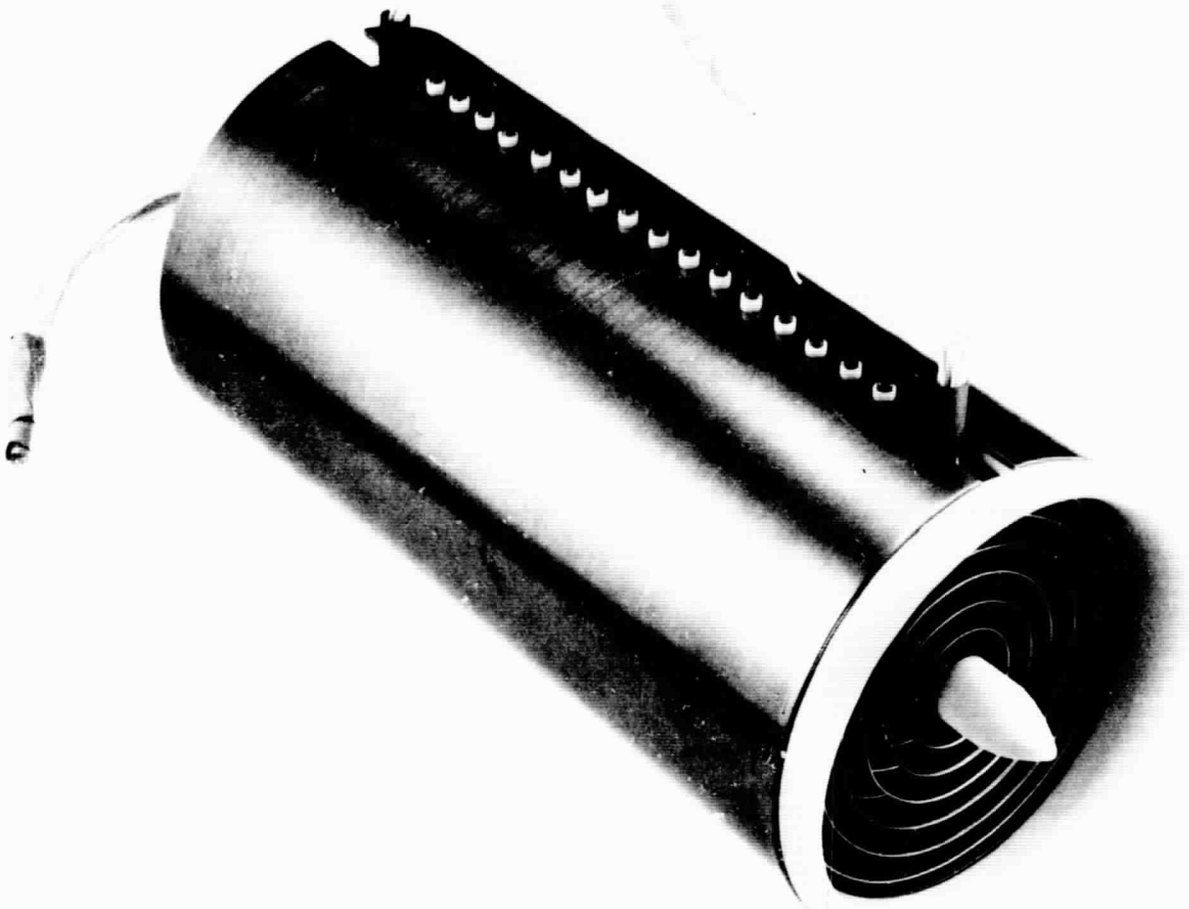

Figure 8 AVCO AC ION MOBILITY SPECTROMETER

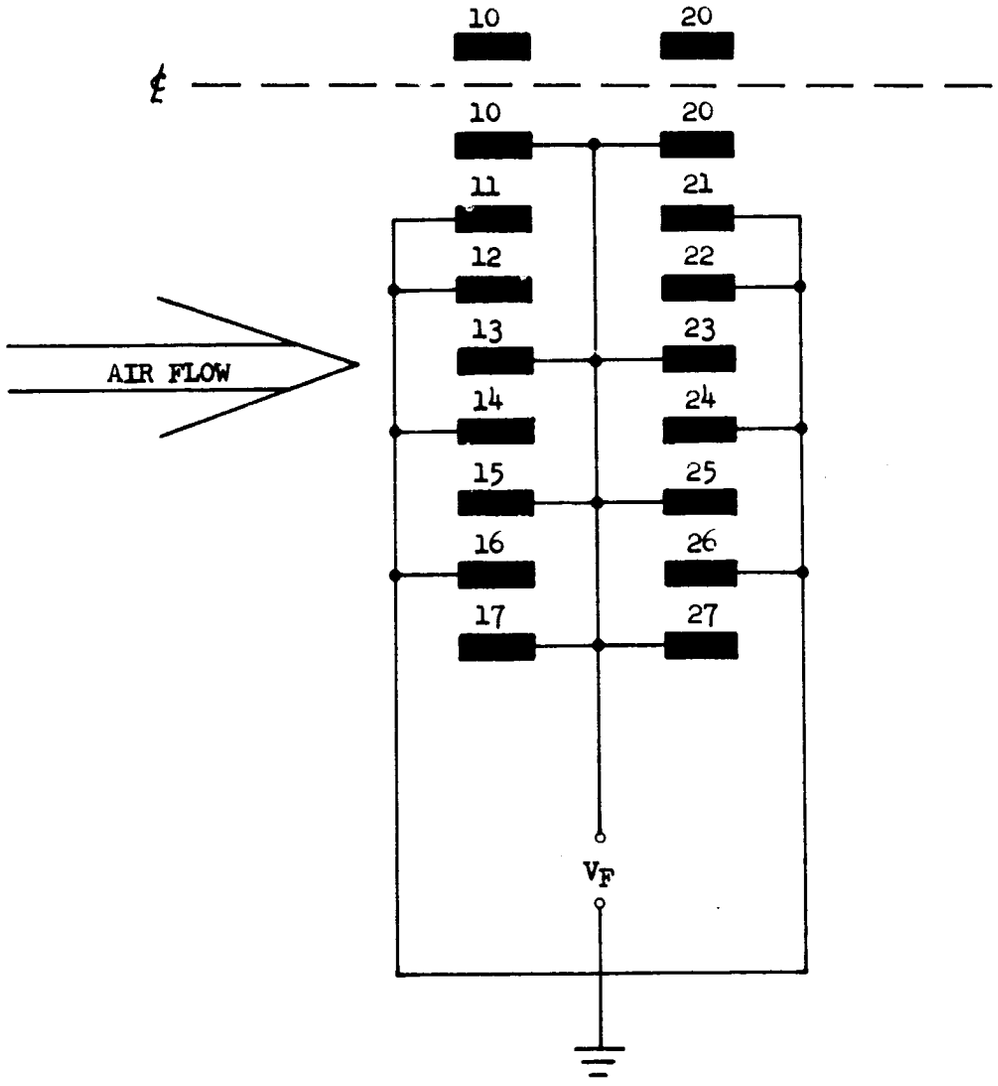

Figure 9 Double Fence with Gate

through which ions may pass. This has the effect of defining the radial coordinate of all ions entering the Gerdien Condenser chamber.

From the analysis of the Gerdien chamber we know that for a particular value of driving voltage, ions having the proper mobility will be collected at a certain collecting electrode. The relationship is

$$X = \frac{v}{k} \quad \frac{\ln\left(\frac{R_C}{R_D}\right)}{2 \quad V_D} \quad \left(R_C^2 - R_G^2\right) \qquad (12)$$

where v is the air flow velocity, k is the ion mobility, V_D is the driving voltage, R_C, R_G and R_D are radii of the collector, gate, and driving electrode respectively, and X is the distance from the plane of the gate to the collector as shown in Figure 10.

The above equation could be written as

$$k = f(V_D, X, v) \qquad (13)$$

This shows more explicitly how the mobility spectrum might be measured. One could hold any two of the variables on the right constant and vary the third, measuring the variation in collected ion current.

In our experiment the easiest procedure was to measure the ion current at a single collector (X fixed) and for a constant pressure and valve setting (v fixed) and vary the driving voltage. This has been done for two cases of velocity-pressure. In each case the measurement was repeated for several of the collectors to determine the self consistancy of the system.

C. Mobility Data

Mobility measurements were carried out at 14 mm pressure in the wind tunnel, which corresponds to an altitude of 27 km The air flow velocity, based on pitot tube measurements is estimated to have been 3 m/sec. The radioactive source was used.

As indicated previously the procedure adopted was to measure the current at one of the 16 collectors of the Gerdien chamber. The air flow velocity was maintained at a fixed value and the driving voltage, V_D, was varied. The curve which resulted is the ion mobility spectrum for air at the particular pressure used. The peak in this curve represents the mobility

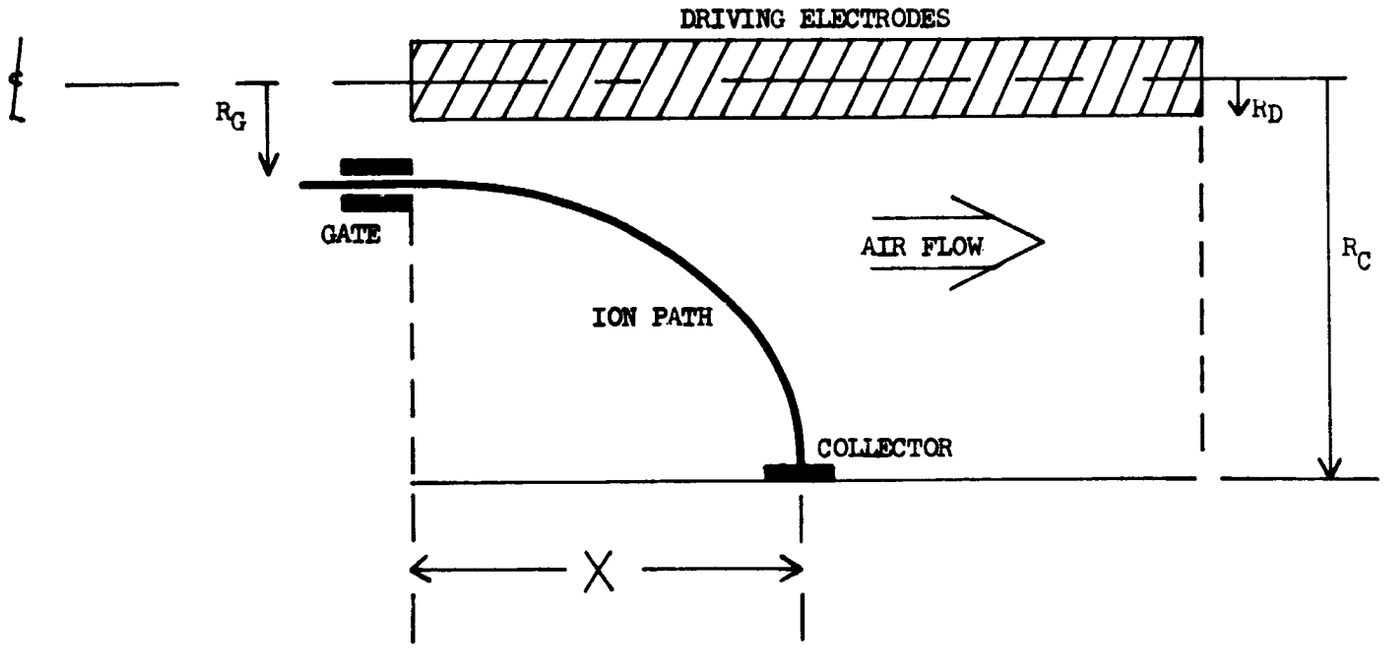

Figure 10 Geometry of IMS

of the most common ion; lower peaks, if they are resolved, represent the mobilities of other ions. The numerical value for each of these mobilities can be calculated from Equation (13) since the parameters V_D and v are measured and the geometrical factors, X, R_C, R_G, and R_D are known. The curve for the first collector (No. 40) is shown in Figure 11.

Additional mobility spectral curves were obtained using other collectors (Figures 11-13). These curves do not in theory contain any new information; they are useful however as a check on the measurement technique. Comparing these curves, a shift in the position of the main peak is seen as one moves from collector to collector. This is predicted by Equation (12) where one sees that for a given mobility the product $X V_D$ is constant. In Figure 14 the value of V_D for the main peak is plotted as a function of $\frac{1}{X}$ (in units of collector number). The approach to the theoretical straight line is remarkably good.

Following an identical procedure, further data were accumulated at a pressure of 0.9 torr (47 km) and an air flow of ~ 14 m/sec. The air was ionized by a corona discharge. As before the mobility spectrum from each collector ring of the Gerdien chamber has been plotted as a function of driving voltage (Figures 15-18). The characteristic shift of the principle peak is again seen in these data. In the plot in Figure 19, fit to a straight line is seen to be excellent.

Equation (12) can be used now to calculate numerical values for a mobility; the geometric factors can be measured and the product $X V_D$ can be taken from Figures 14 and 19 for each of the altitudes. The mobilities represented by the principle maxima of the experimental spectra turns out to be, at 27 km -- 1.2×10^{-2} $\frac{m^2}{v\,sec}$ and at 47 km -- $6.6\ 10^{-2}$ $\frac{m^2}{v\,sec}$. In the report by Dolezalek and Oster (1965) a table of calculated values for mobility at various altitudes will be found. These values are used to plot the curve in Figure 20. The two experimental points in this figure are the results of our application of Equation (12). A range of confidence is shown which is based on an estimate of the accuracy of the velocity measurement.

D. Resolution

A question should be raised to the structure one might expect to see in these mobility spectra. The structure will depend upon the variation in mobility for different ion species and on the effective resolution of the spectrometer. From the mobility theory of P. Langevin as modified by others we see that the mobility is

$$k \sim \sqrt{\frac{M + m}{m}} \qquad (14)$$

Figure 11. Ion Mobility Spectrum Collectors No. 40-42

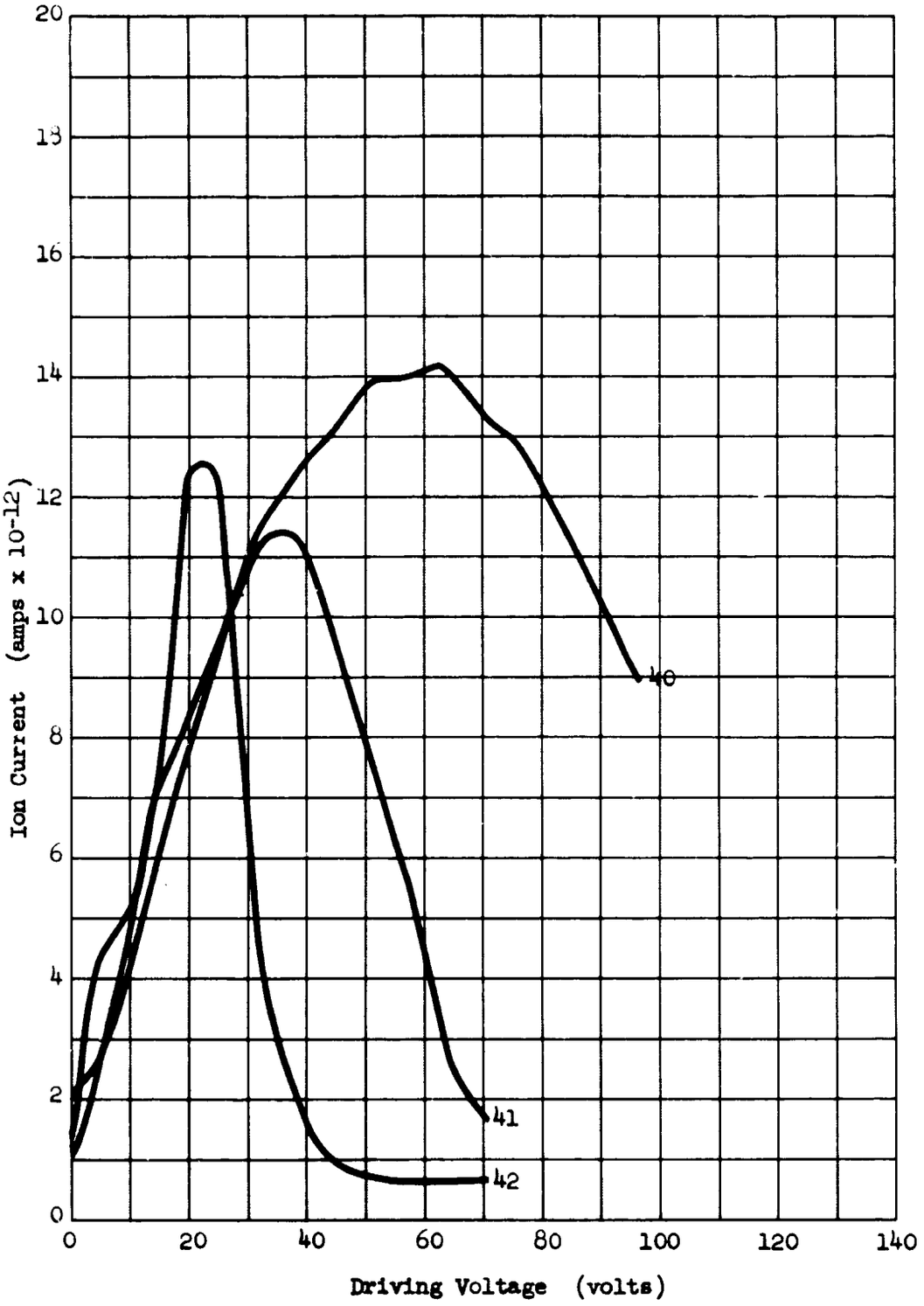

Figure 12. Ion Mobility Spectrum Collectors No. 43-47

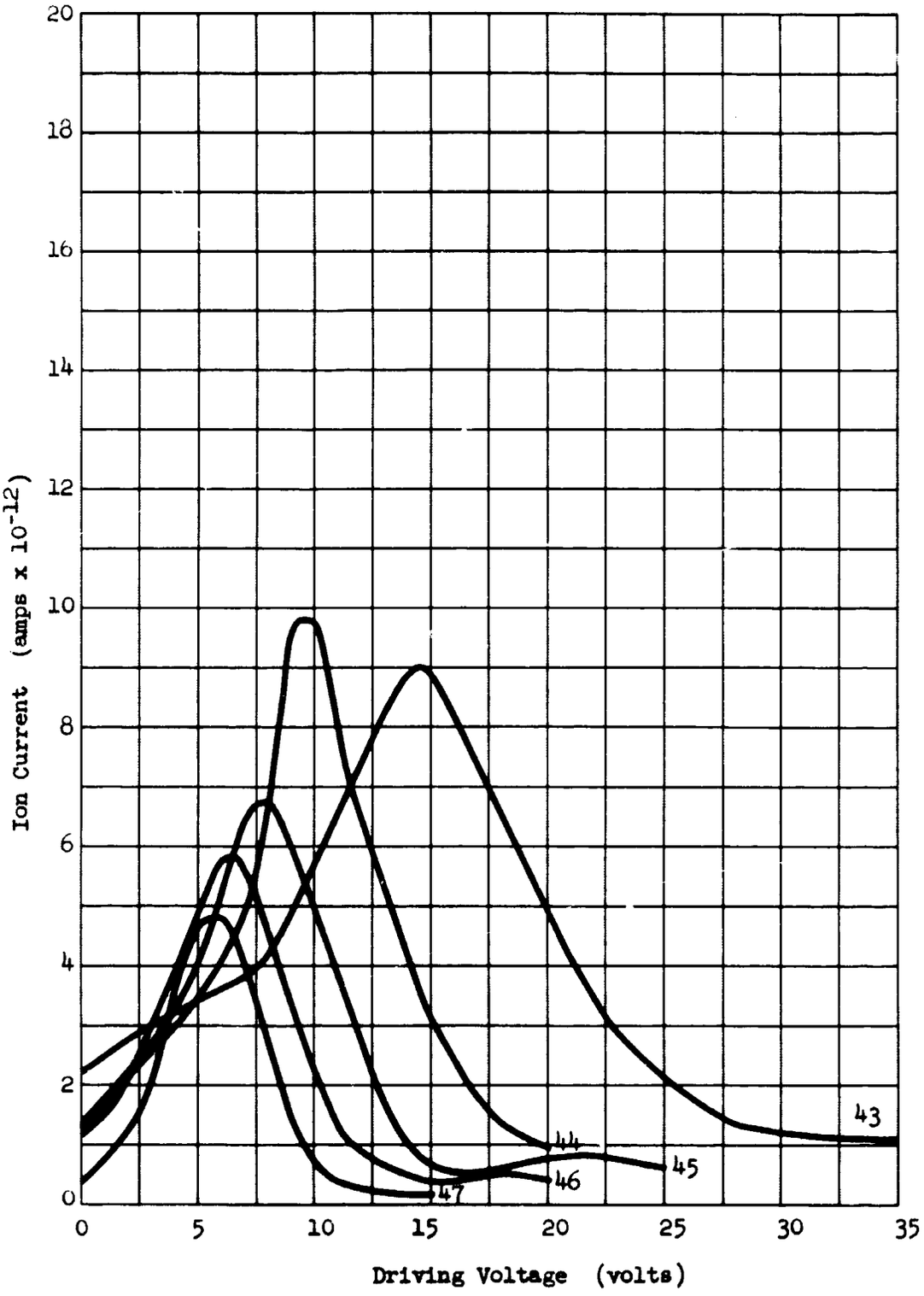

Figure 13. Ion Mobility Spectrum Collectors No. 48-55

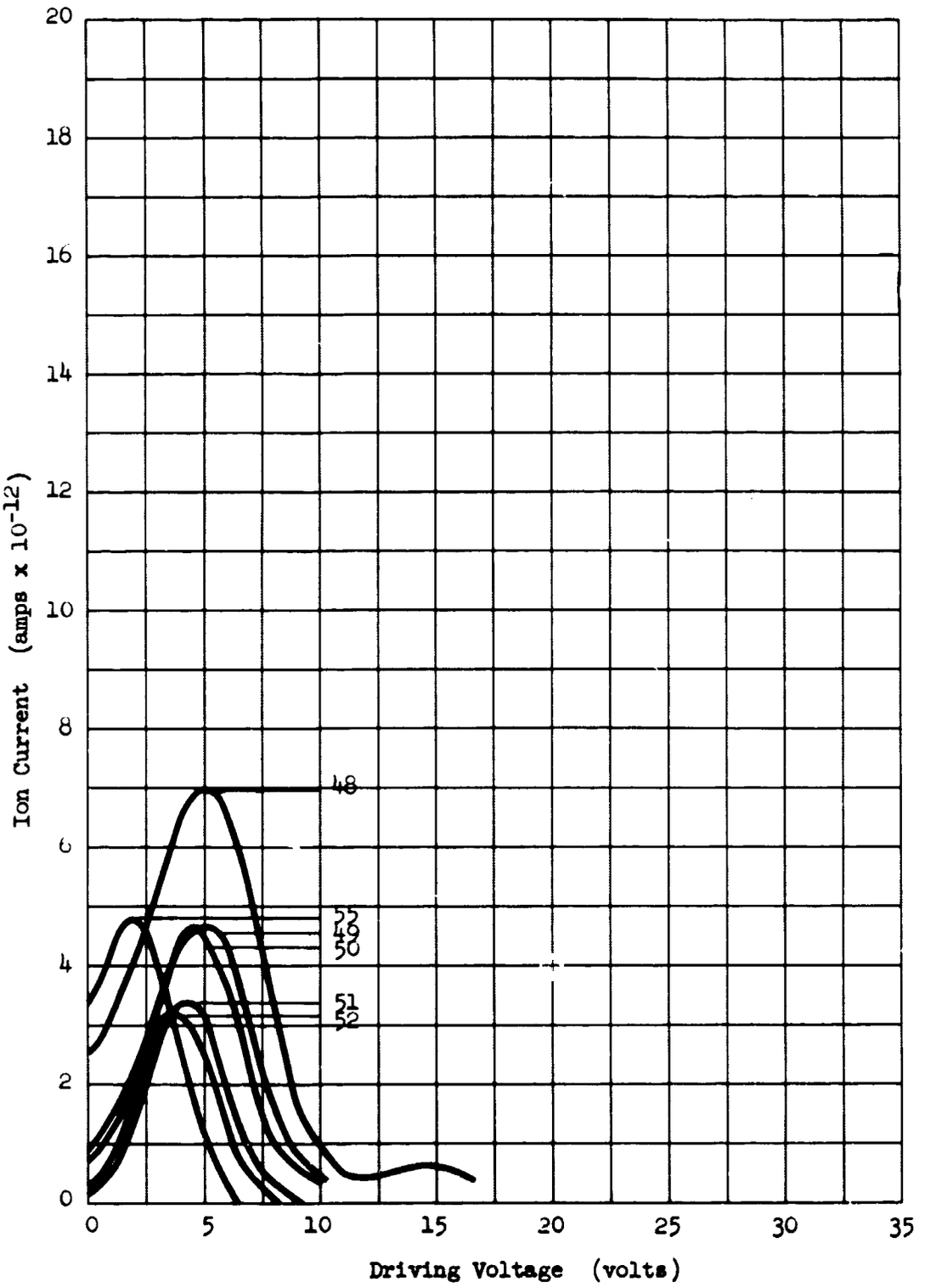

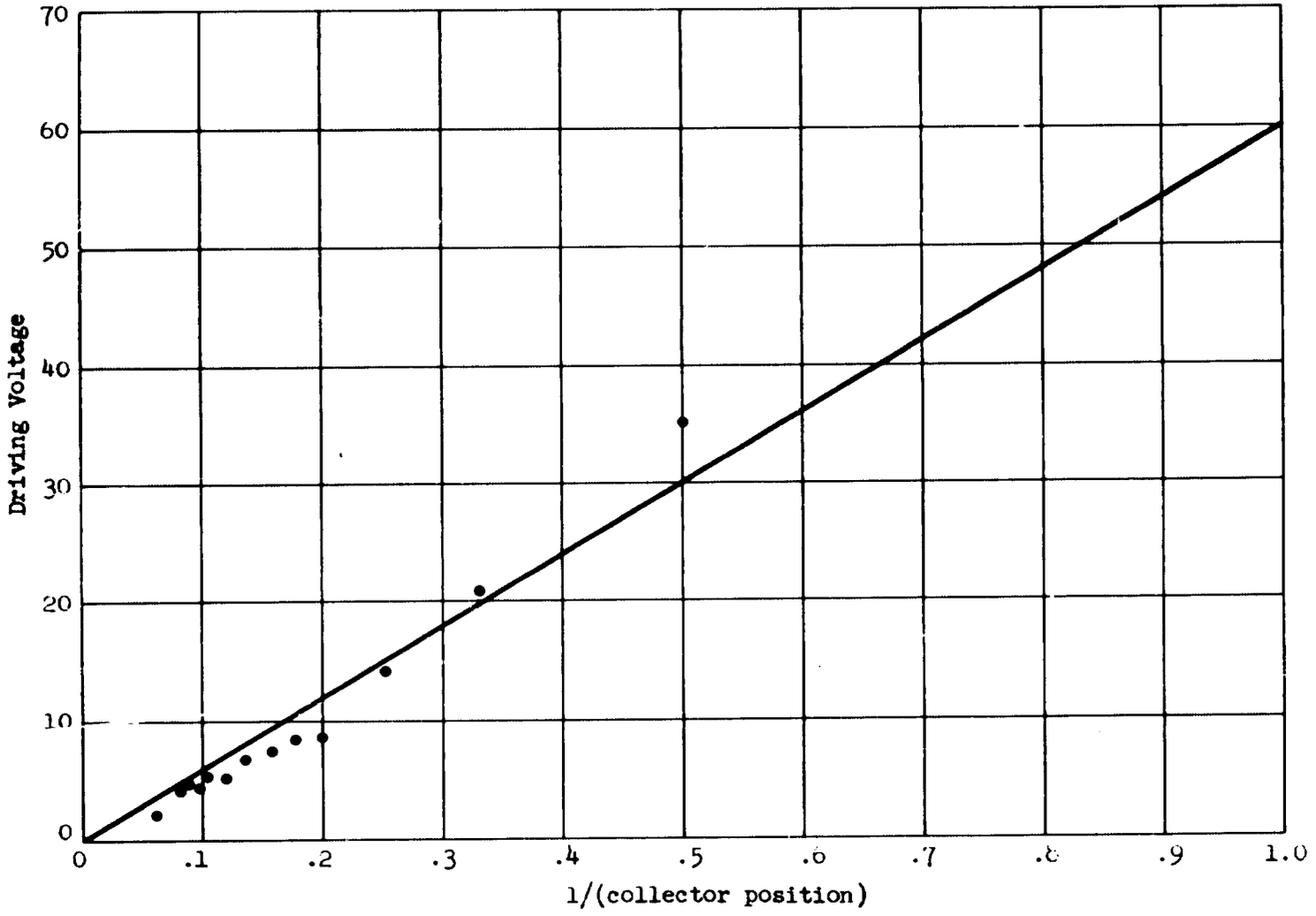

Figure 14. Spectrum Peak Shift

Figure 15. Ion Mobility Spectrum Collectors No. 40-41

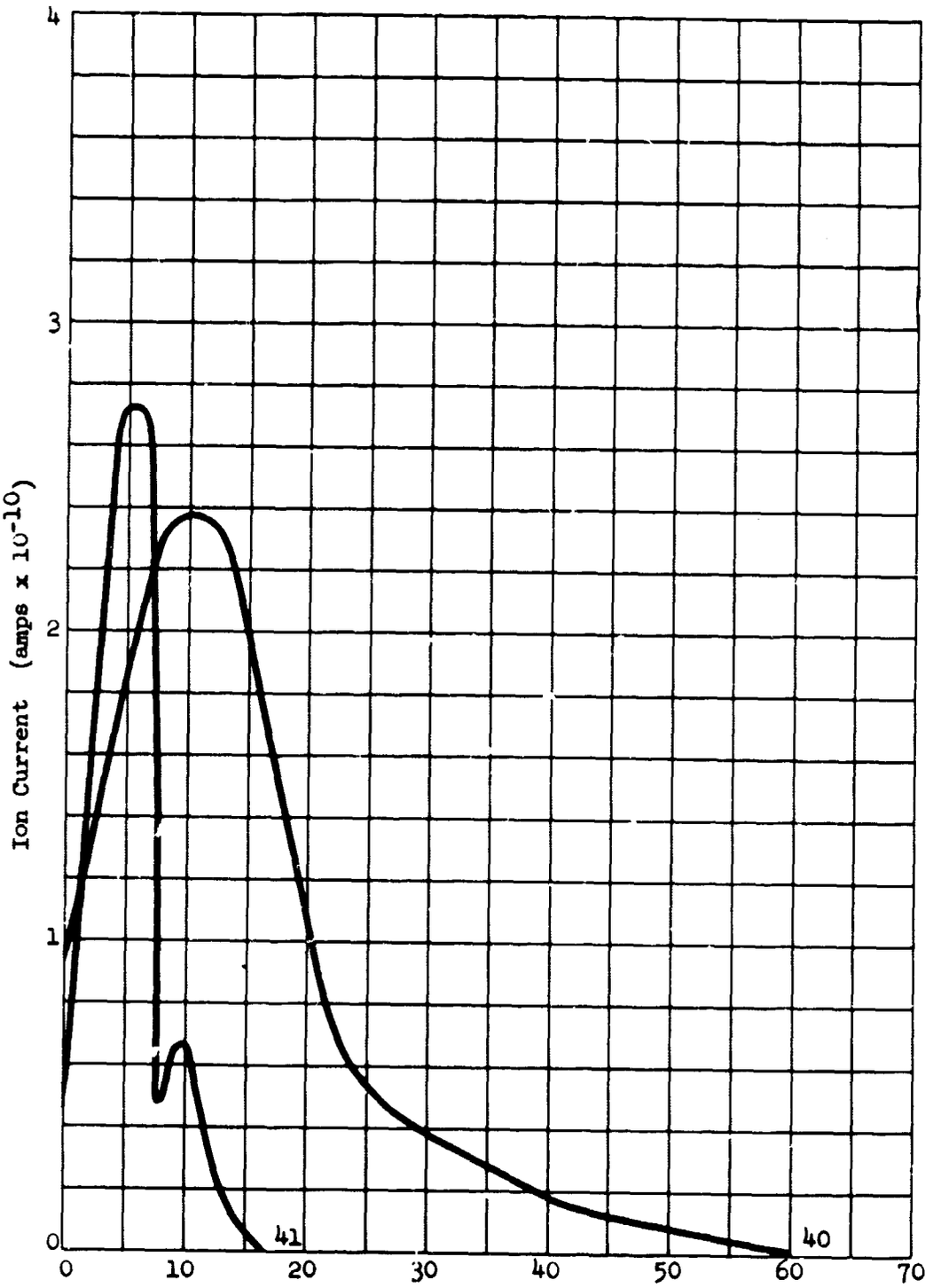

Figure 16. Ion Mobility Spectrum Collectors No. 42-44

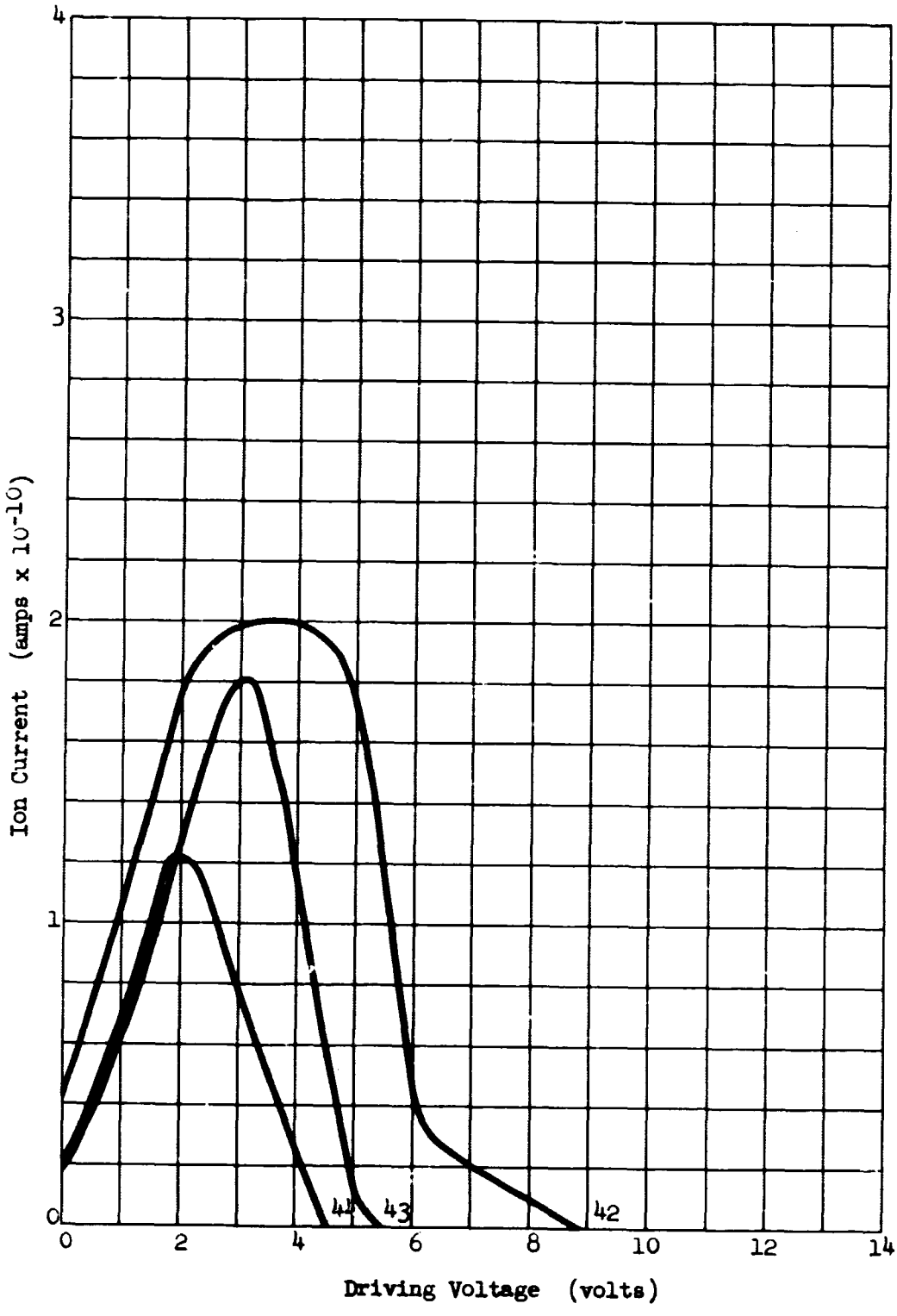

Figure 17. Ion Mobility Spectrum Collectors No. 45-50

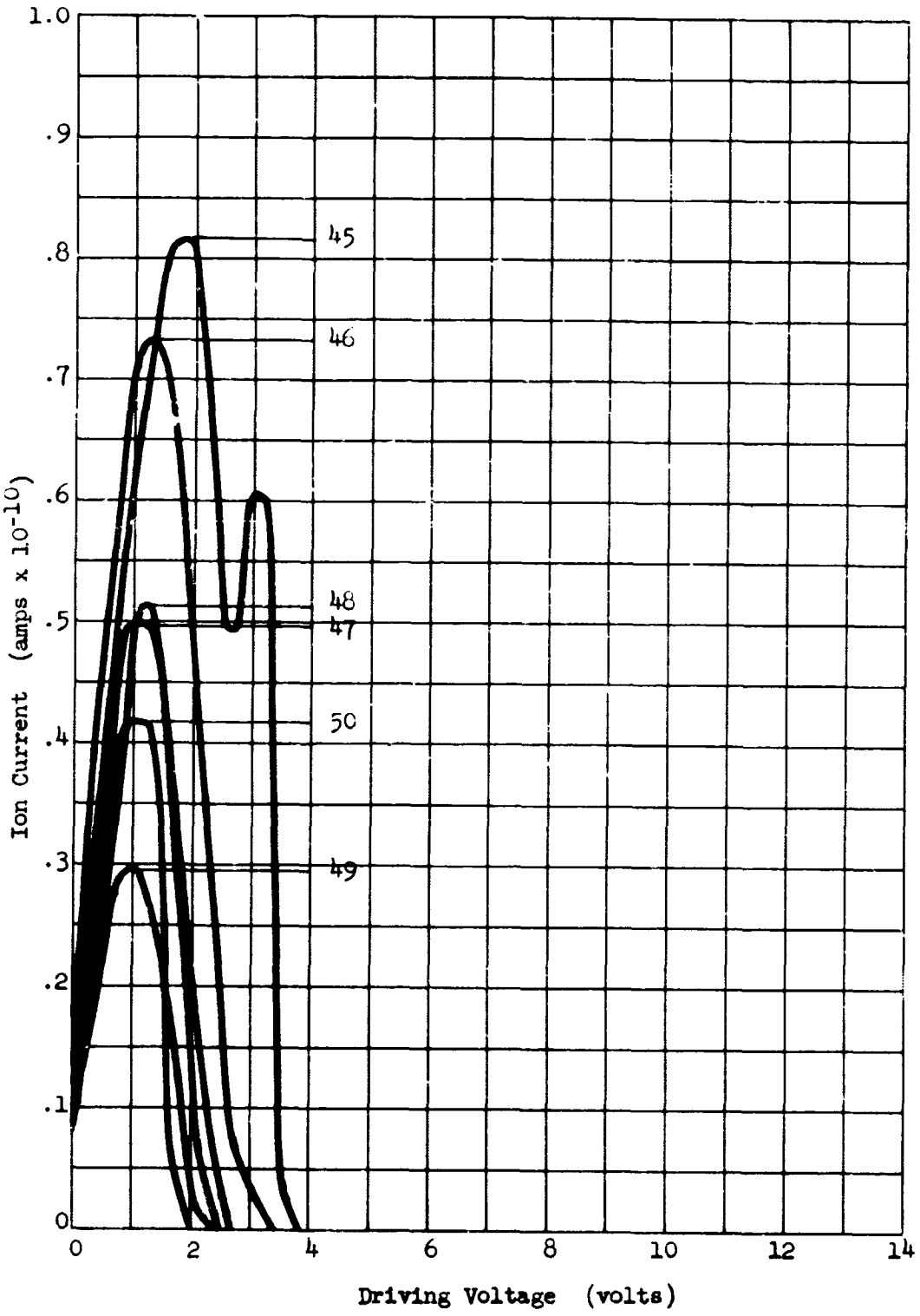

Figure 18. Ion Mobility Spectrum Collectors No. 51-55

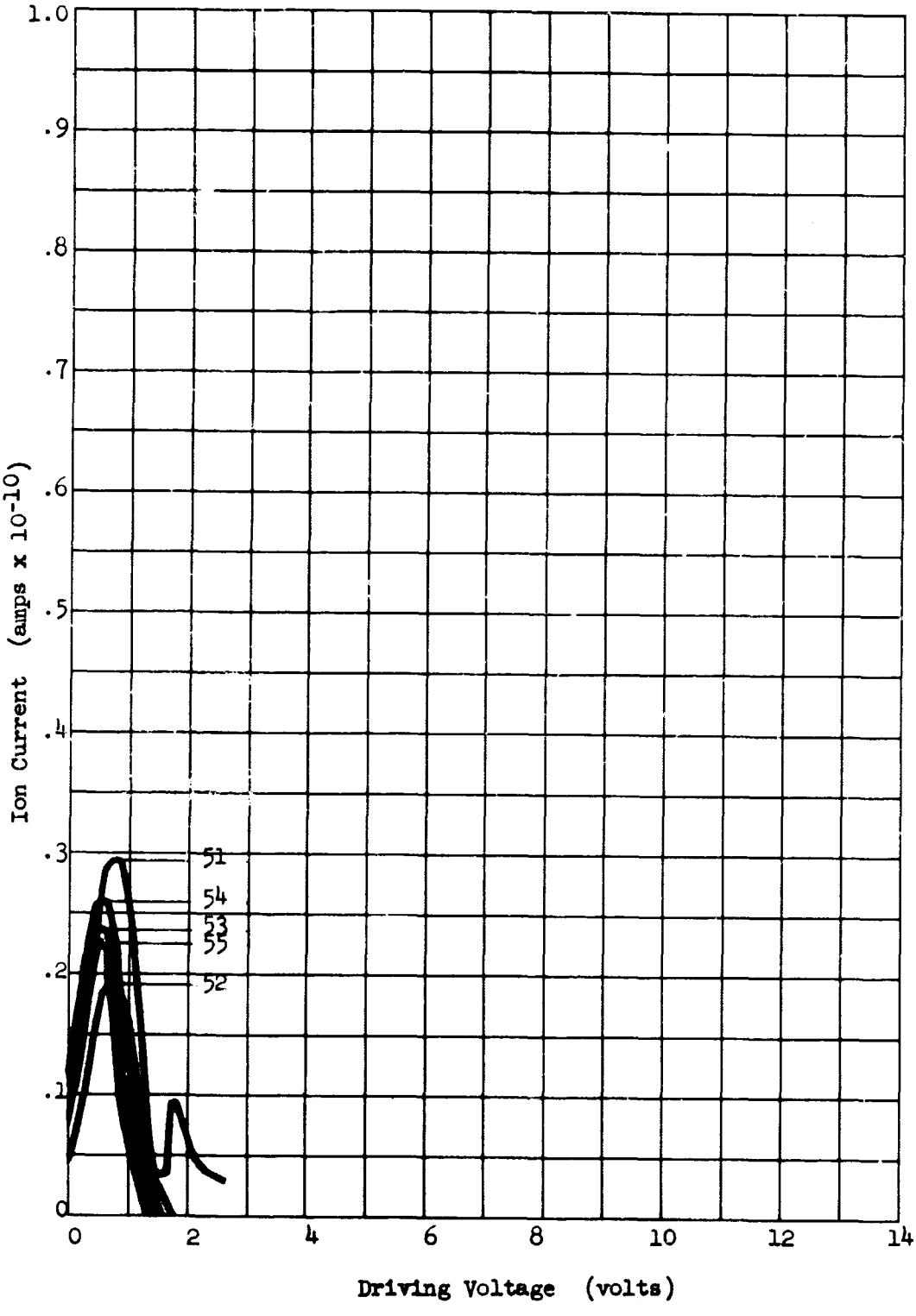

Figure 19. Spectrum Peak Shift

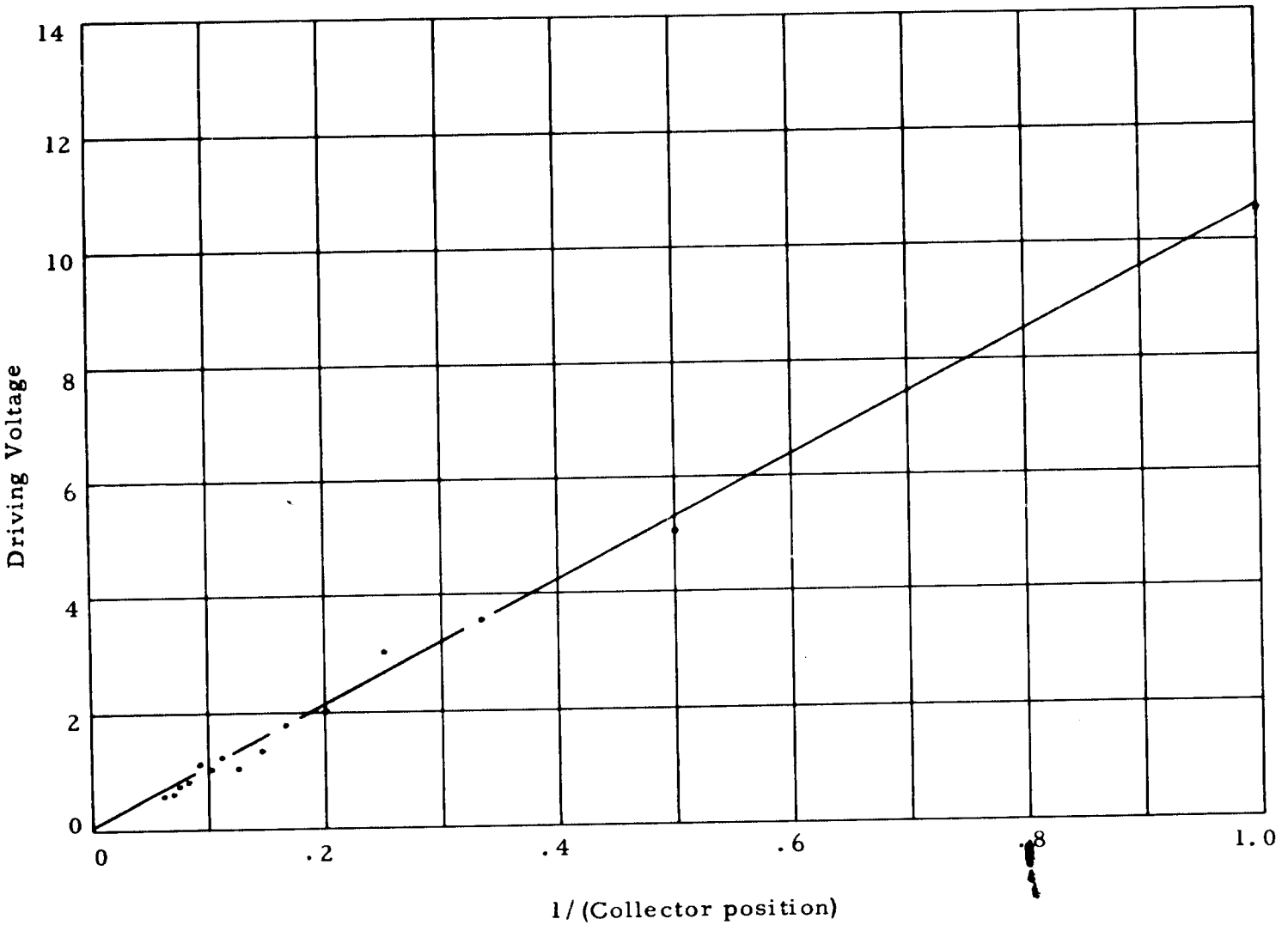

Figure 20. Plot of Ion Mobility vs. Altitude

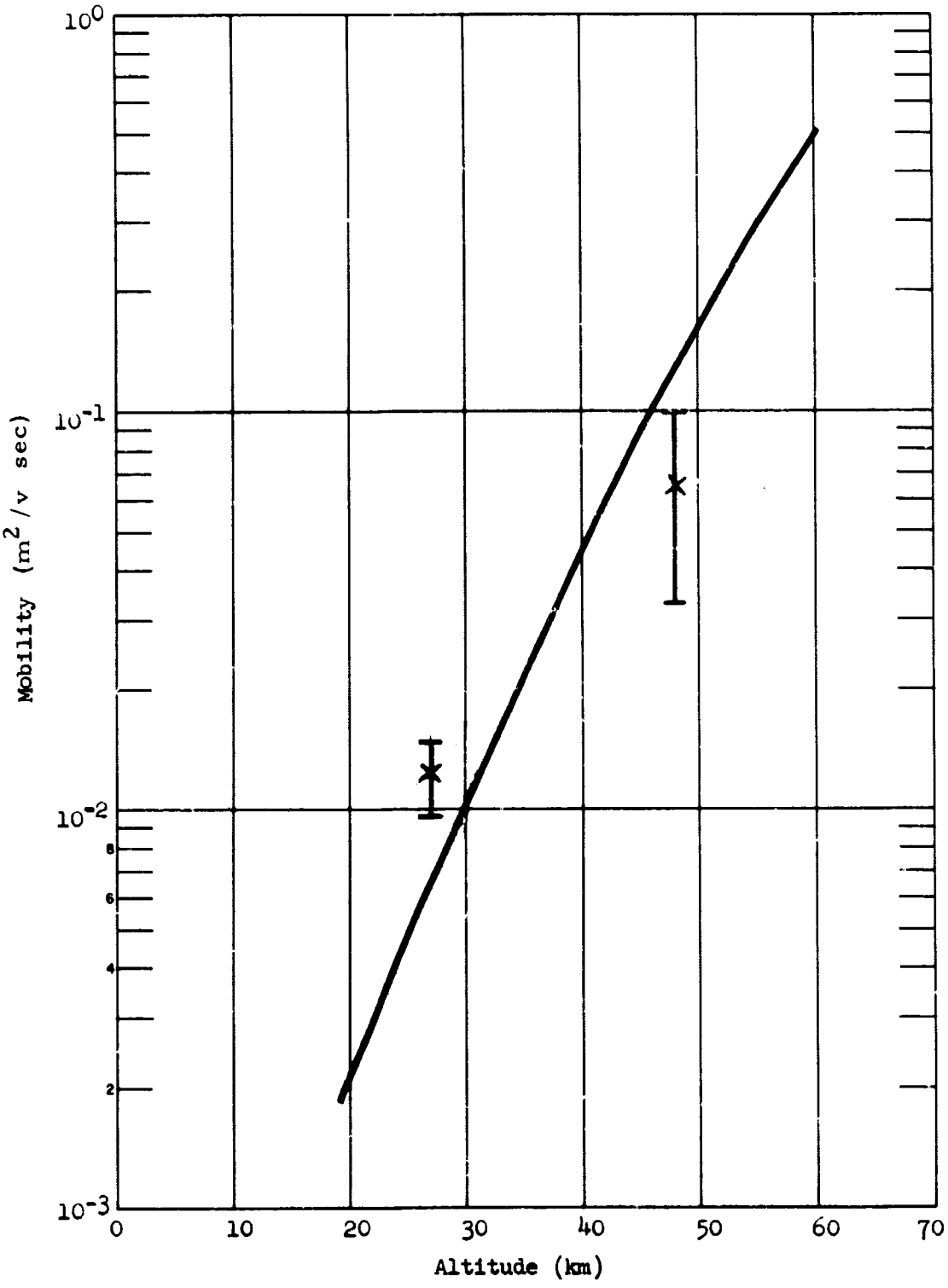

where M is the molecular weight of the neutral gas and m is the molecular weight of the ion. Using this formula one finds that the mobilities for mass 18 and 28 ions (in air) differ by about 12 percent.

From the analysis of the Gerdien chamber we know that for a particular value of driving voltage, ions having the proper mobility will be collected at a certain collecting electrode. The relationship is

$$k = \frac{v}{x} \quad \frac{\ln\left(\frac{R_C}{R_D}\right)}{2\ V_D} \left(R_C^2 - R_G^2\right) \qquad (15)$$

where v is the air flow velocity, k is the ion mobility, V_D is the driving voltage, R_C, R_G, and R_D are the radii of the collector, gate, and driving electrode respectively, and x is the distance from the plane of the gate to the collector. This is of course just an inverted form of Equation (12).

The contribution to the uncertainty in mobility, Δk, is due to an uncertainty in each of the observables and can be calculated using the partial derivatives from Equation (15).

$$\Delta k_x = \frac{\partial k}{\partial x} \Delta x \qquad (16)$$

Similar expressions can be written for v, V_D, R_C, R_D, and R_G. The total uncertainty Δk is taken to be

$$\Delta k = \sqrt{\sum (\Delta k_i)^2} \qquad (17)$$

The error which may arise due to three of the variables is quite small since V_D, R_C, and R_D can be measured accurately. The uncertainty in R_G is inherent to the design of the IMS and is equal to one half the distance between the two rings which form the gate. This gate half-width could be reduced but this would diminish the signal available from the IMS. Δk_{R_G} turns out to be 0.043 k for our geometry.

The uncertainty in x is due to the width of the collector rings and varies from 100 percent for the first collector to 33 percent for the second, 20 percent for the third, 6.6 percent for the eighths, and 3.2 percent for the sixteenth. We will take $\Delta k_x = 0.143$ k (fourth collector) for this discussion.

The uncertainty in air flow is high, 30 to 50 percent, in that the instrument used to measure this parameter is uncalibrated. However, the high stability and reproducibility of the velocity measurements suggests that fluctuations are

small. In a determination of the resolution of the system, stability and not absolute accuracy is the important consideration; we estimate $k_v = 0.05\ k$. From Equation (17) we can calculate the total uncertainty

$$\Delta k = 0.16\ k.$$

On comparison of this result with the calculated peak separation of 12 percent (based on molecular weights) between mass 18 and mass 28 one would not expect good separation of these peaks but should not be surprised to see indications of multipeaked structure in the mobility spectra. This is how our data have been interpreted. (See Figure 17 for example).

V. MASS SPECTROMETER

A. The Quad 150A

Two quadrupole mass spectrometers were used in this research program. The first, made by AFCRL was loaned to us through the generosity of Dr. R. Narcissi. The instrument was of the type designed by him for rocket flight experiments. The operating principles and general configuration were similar to those of a Quad 150A residual Gas Analyzer subsequently obtained from GSFC. The descriptive material on the Quad 150A (manufactured by Electronic Associates Inc., Palo Alto, California) is contained in the EAI Instruction Manual.

The trajectory of an ion in a quadrupole field is defined by a Mathieu equation in which $\beta = V_1/V_o$ is a parameter. V_1 is the DC amplitude and V_o is the RF amplitude of the voltage applied to the quadrupole rods. The stability of the solution is given in Figure 21. Notice that as $\beta = V_1/V_o$ approaches approximately 0.168, the range of values which α can assume and still have the ion's trajectory stable becomes more and more limited. In conventional mass spectrometer terminology, as β approaches 0.168, the resolution of the instrument increases.

A further consequence of Figure 21 is dependence of ion mass on β. If β is held constant and V_o is varied, then the value of e/m for which the trajectory is stable will change with V_o. Since $\beta = V_1/V_o$, V_1 must also be varied. To sweep the mass range from 1 AMU to 150 AMU, V_o is varied from zero to 200 volts. The circuitry is such that two rods go to +200 volts and the other two rods go to -200 volts. Thus the axis remains at ground. This is an important consideration for the next topic, ion optics.

B. Ion Optics

The elements of the Quad 150A are shown in Figure 22. In the normal mode of operation, ions are created within the Faraday Cage which is at a potential of +11 volts. The Focus Lens is normally at -90 volts and the Exit Lens is at ground. We have already pointed out that the filter rods are at $\pm V_o$ so that the Z-axis is also at ground. The first dynode of the electron multiplier operates at -3 KV. From these values one can see that a positive ion will enter the filter with 11 ev kinetic energy and hence a velocity along the Z-axis. The ion will drift through the filter with this constant velocity until it enters the multiplier and is accelerated into the first dynode. It is clear that negative ions generated by the electron beam in the ionizer cannot travel this path. Also, if the kinetic energy were zero there would be no Z-component of velocity and even positive ions would fail to reach their goal.

In Section III.B, it was stated that the mass spectrometer differential pumping system was reduced from three chambers to a single chamber to

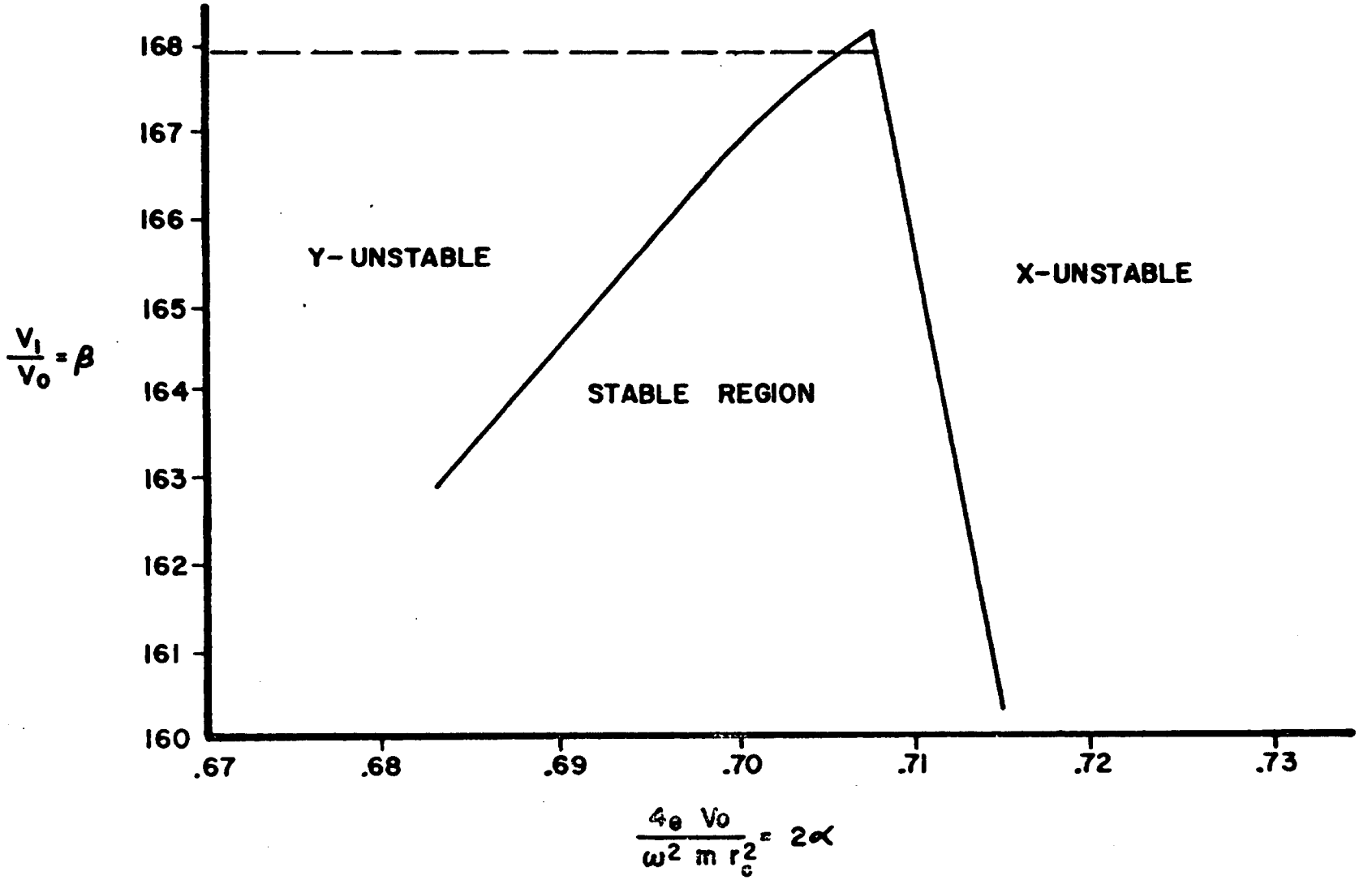

Figure 21 STABILITY DIAGRAM

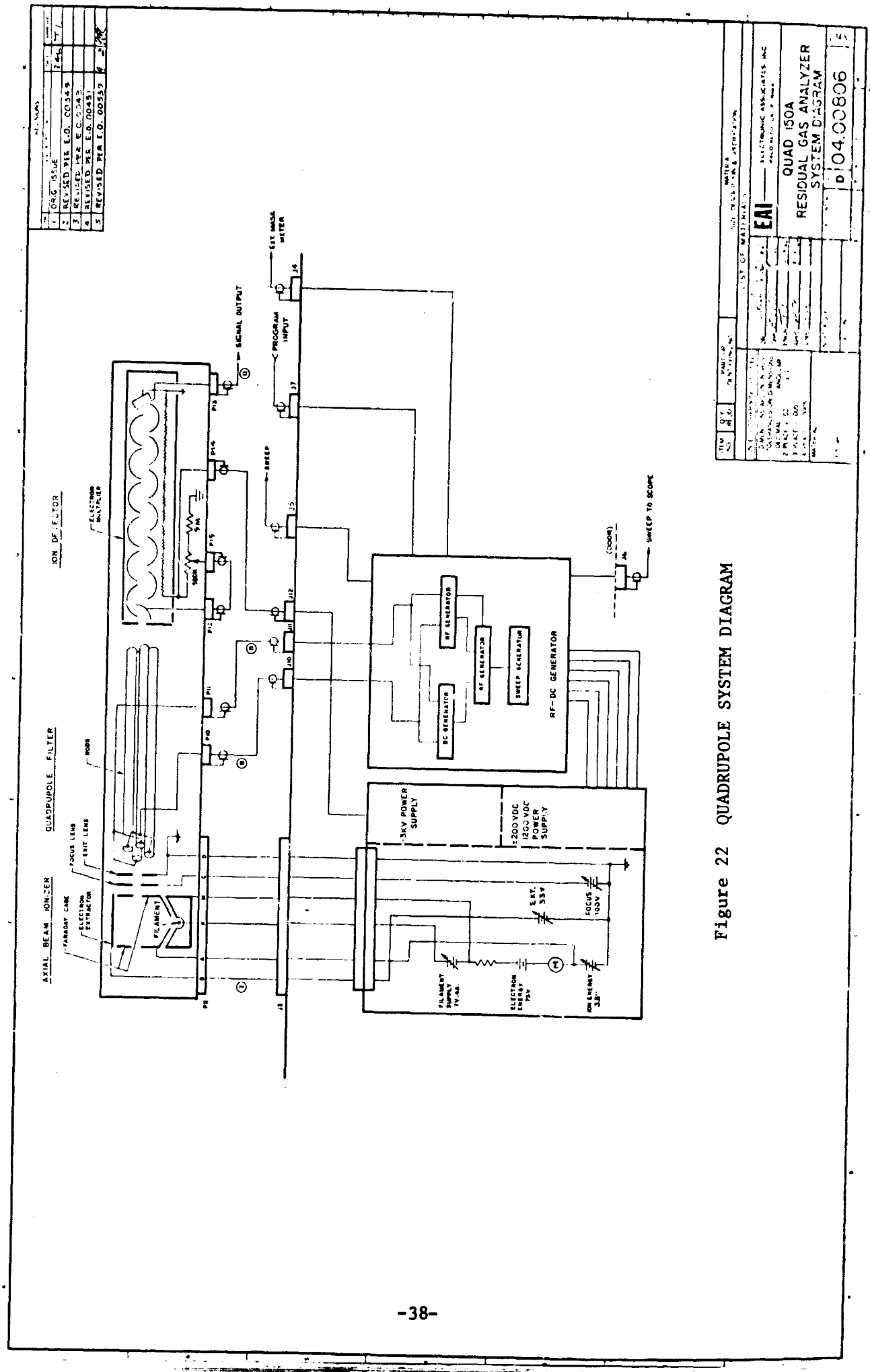

Figure 22 QUADRUPOLE SYSTEM DIAGRAM

reduce the loss in ion density which was apparently taking place. With the single chamber a signal, albeit very small, was seen.

A further refinement was then made. A three element electrostatic lens, as indicated in Figure 5, was designed and installed in the differentially pumped chamber between the entrance hole and the mass spectrometer. A photograph of the lens mounted on the entrance hole flange is shown in Figure 23. The lens focused the ion entering from the wind tunnel onto the entrance of the quadrupole and had the effect of increasing the signal strength by nearly an order of magnitude. In Figure 24 the mass spectrum of air is shown. The tunnel pressure was 32 μ and the air was ionized by a 1.5 KV corona discharge. Peaks have been identified with mass numbers. A second spectrum is shown in Figure 25. In this case dry nitrogen gas (not air) was bled into the wind tunnel. The pressure was 70 μ and a 2 KV corona discharge was used to ionize the gas. As would be expected, only the mass 28 peak appears. These data were taken with the AFCRL quadrupole mass spectrometer. The entrance hole plate and the first plate of the lens were at +20 volts; plate two was at +51.5 volts; plate three was at +40 volts. By operating the entrance hole plate at a positive potential the necessary axial ion velocity in the filter was assured.

When the vacuum system was modified to accept the Quad 150A, the electrostatic lens was also adapted to the new housing. Although the lens appeared to be less effective than before, mass spectra were observed if the entrance hole plate was at +75 volts or more. Because of the relatively high positive voltage required at the entrance hole plate and because the spectrometer response increased with increasing applied voltage at that point, it was speculated that some secondary effect might be taking place and that the spectra were not due to entering positive ions alone.

Observations were made which proved a positive correlation between the detection of positive ions with the Quad 150A, and corona discharge current and air flow velocity. It was also found that the Quad 150A output could be controlled by the Gerdien chamber. The Gerdien was placed between the corona source and the mass spectrometer. With all Gerdien electrodes grounded a mass spectrum was observed. As the driving voltage in the Gerdien was increased the collected current increased and the spectral peak heights decreased.

Two mechanisms are put forward as tentative explanations of the observations just described. The plasma generated by the corona discharge is neutral and very dense. Because weak external fields cannot penetrate such plasmas the potential of the entrance hole plate has little effect on the external (high pressure) side. On the low pressure side the expanded gas behaves quite differently, with the positive ions now accelerated into the the quadrupole aperture.

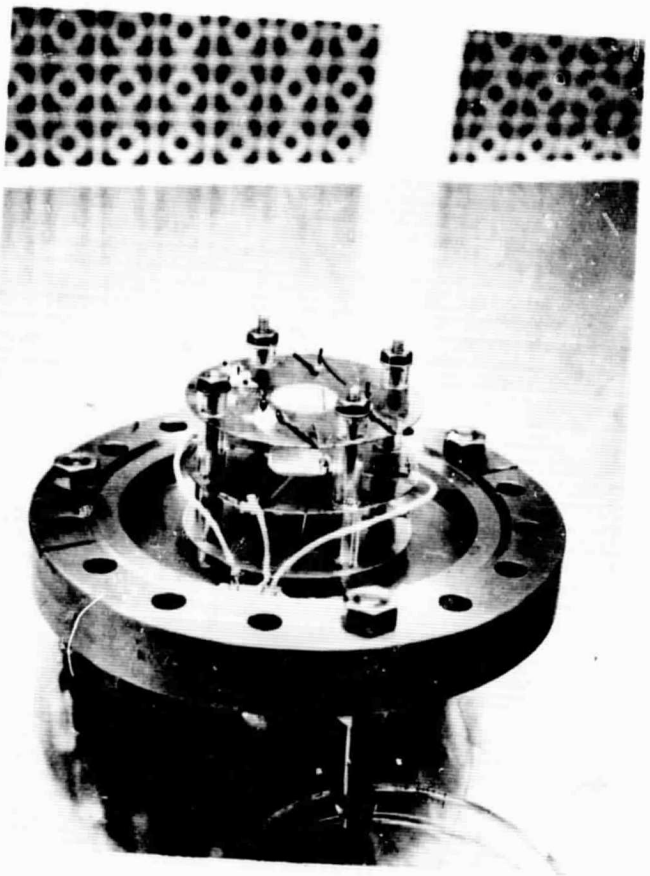

Figure 23 Ion Lens

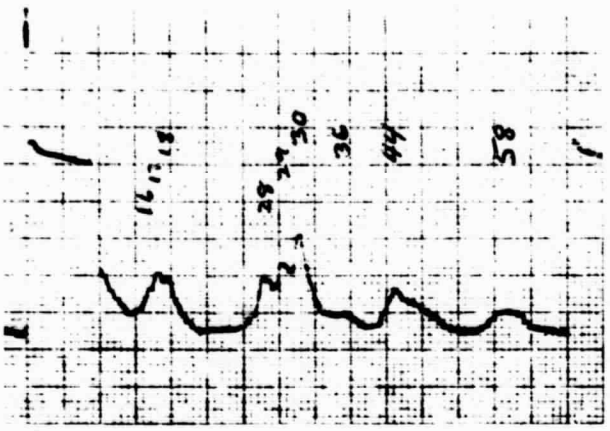

Figure 24

MASS SPECTRUM - AIR

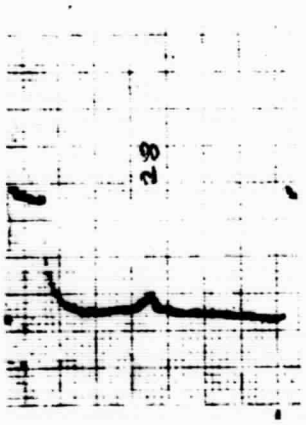

Figure 25

MASS SPECTRUM - NITROGEN

The alternative mechnism calls for a secondary ionization to occur just inside the entrance hole at a point where fields and gas pressure happen to be correct. This ionization is triggered by the small number of charged particles which enter from the corona generated plasma. Some further measurements were made to enlarge our understanding of the ion trajectories. We are, however, unable to determine which, if either, of the processes described is correct.

C. Concurrent Measurement of Mass and Mobility Spectra

A series of measurements were made with the Gerdien chamber and the Quad 150A operating together. It has been noted that the intensity of the mass peaks could be controlled by the Gerdien driving voltage. This effect is shown in Figure 26. The variation in the intensity of the two principal peaks, mass 18 and mass 28 is shown. The complete mass spectrum, for zero Gerdien voltage, is reproduced in Figure 27. For these data, the wind tunnel pressure was .88 torr which corresponds to an altitude of 47 km; the air flow velocity was 22 m/sec. As in earlier low pressure measurements, a corona discharge of one kilovolt was used to ionize the gas.

Mobility spectral curves of the type presented in Section IV-D were recorded and one of these is shown in Figure 28. One can see two peaks in this curve; the more intense has the lower mobility. In the mass spectrum the more intense peak was mass 18, the lower mass.

There would seem to be a contradiction here since the theoretical model of mobility states that

$$k \sim \sqrt{\frac{M + m}{m}} \qquad (14)$$

It is suspected that with additional data which will result from the proposed study of ion optics, the apparent conflict will be resolved. Variation of the wind tunnel gas composition will assure this end.

D. Plasma Measurements

At the close of the contract, two measurements were made in an attempt to broaden our understanding of the significance of the observed mass spectra. It is crucial to show that these spectra represent the relative ion concentration in the wind tunnel and are not due to ions created in the vacuum region of the quadrupole. In Figure 29, the results of a measurement of current to the entrance hole plate is shown. A battery was placed between the plate and a Keithley pico-ammeter so that the plate bias could be varied between plus and minus 200 volts. For a negative bias, a positive current due to positive ions is seen. When the bias is reversed, negative carriers are collected. The dependence is approximately linear for bias voltages less than about +100v

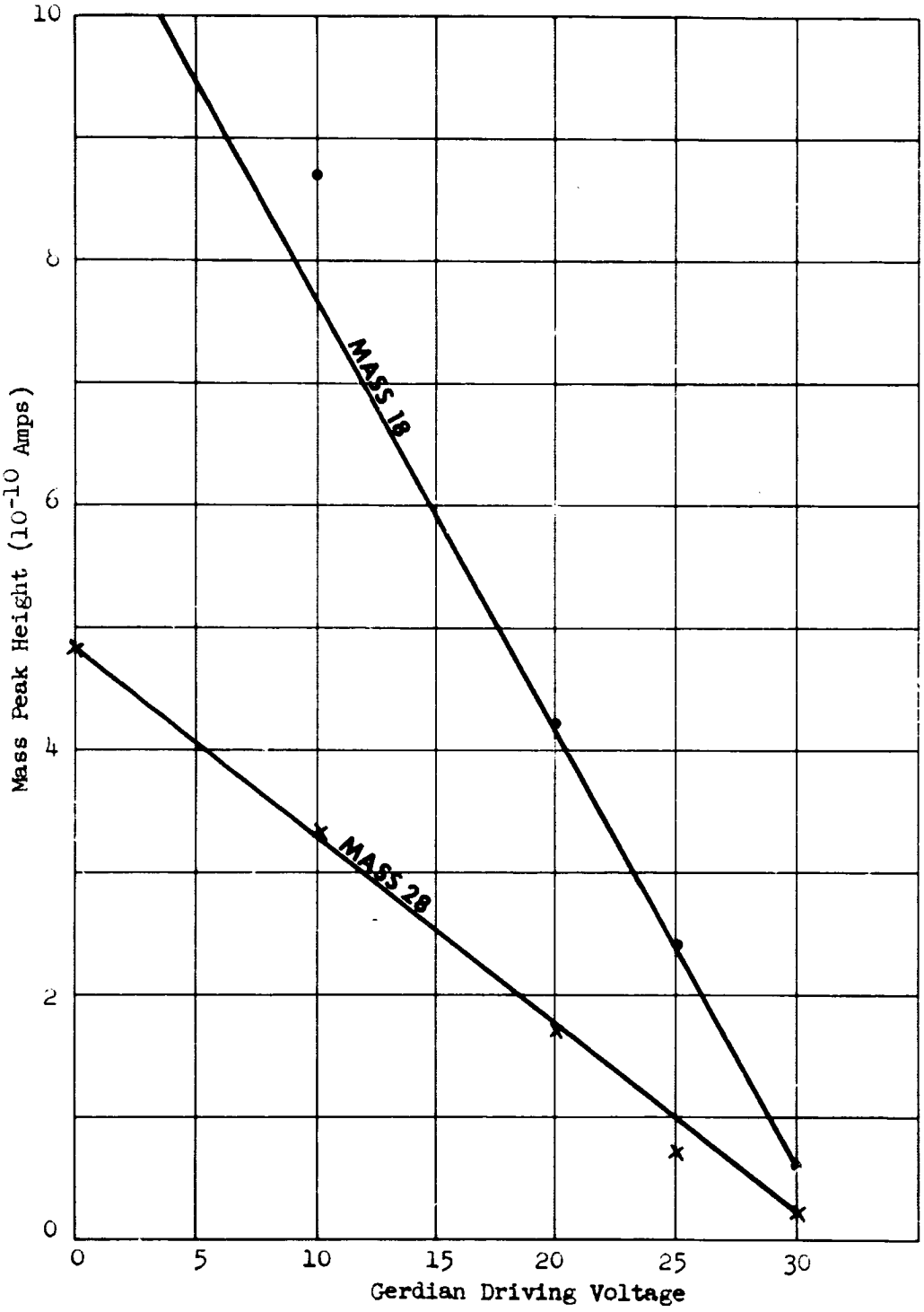

Figure 26. Effect of Gerdien Voltage on Observed Mass Spectrum

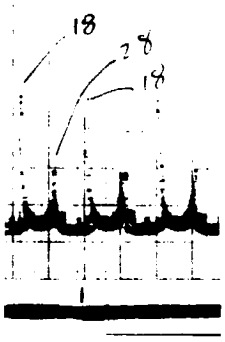

Figure 27

Mass Spectrum - Air

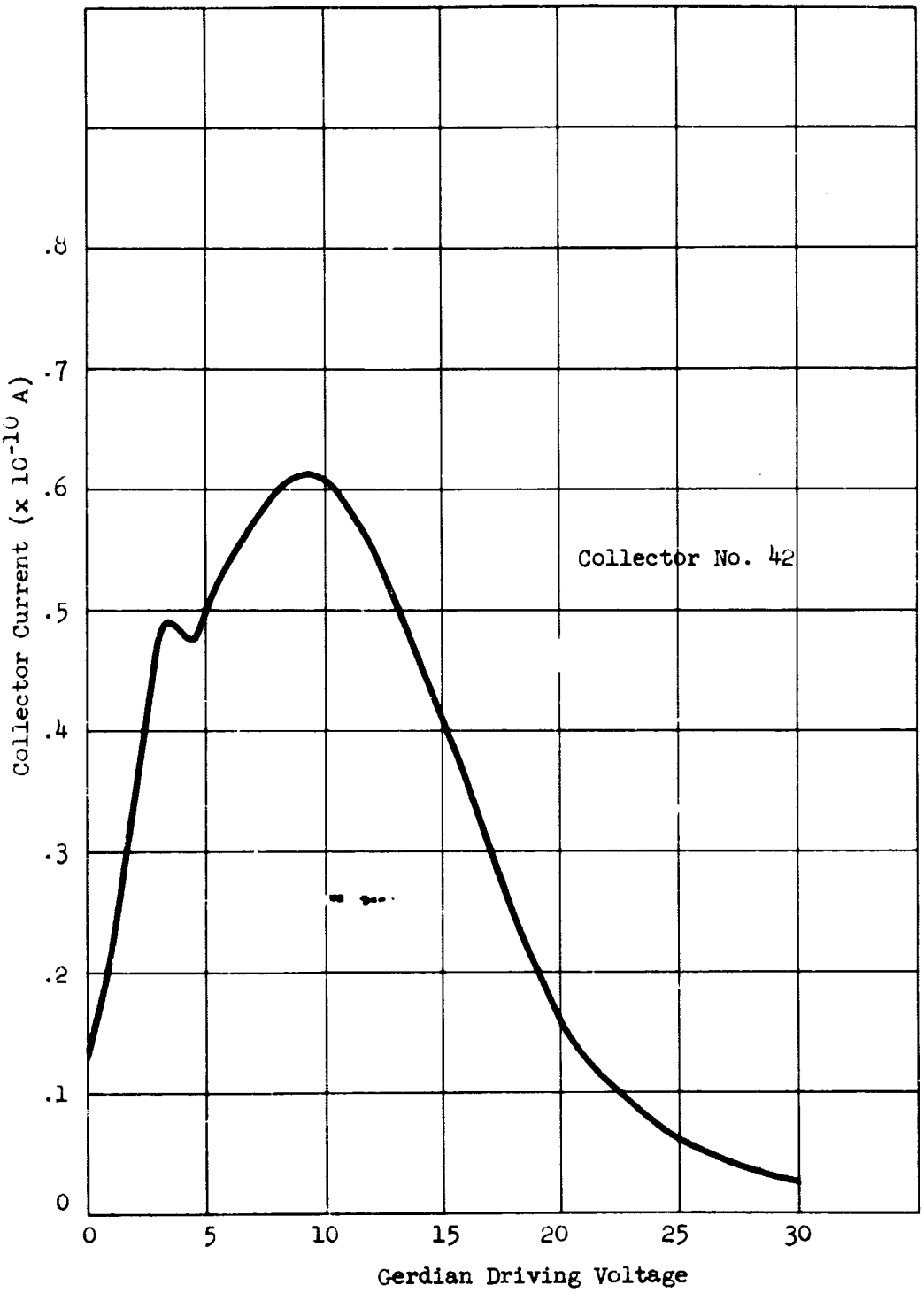

Figure 28

Mobility Spectrum - Air

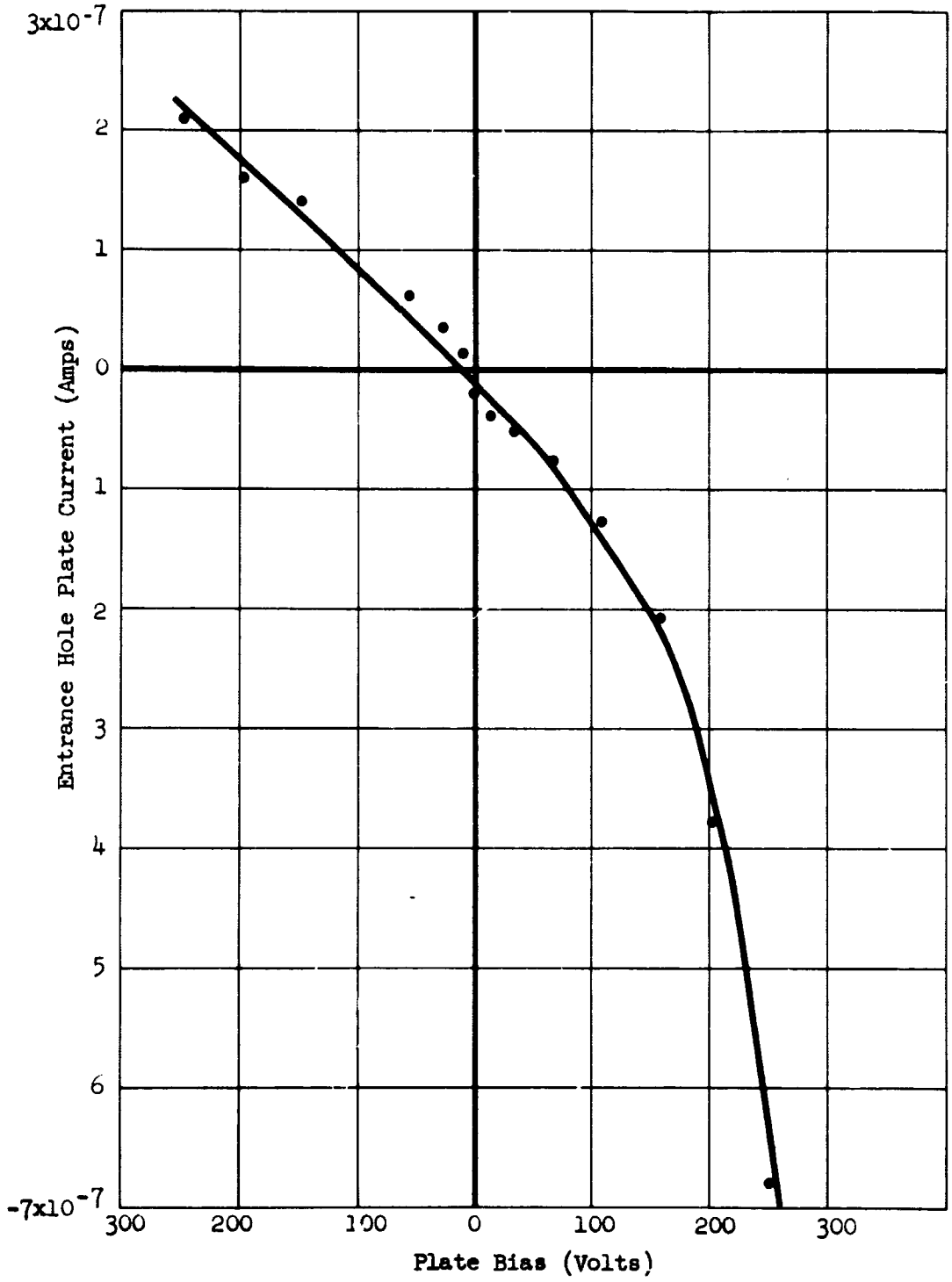

Figure 29

Entrance Hole Plate Current Variation

at which point an avalanche appears to start. (The diameter of the entrance hole plate is 1.5 inches). These measurements were conducted at a wind tunnel pressure of 300 microns, a flow velocity of about 25 m/sec, and with the corona source operating at -500 v. The ion density is estimated to be 10^7 per cm^3.

For the second measurement a screen was placed inside the entrance hole to collect the transmitted ions. The plot in Figure 30 shows how the screen current varied with entrance plate voltage for a fixed bias of -55 volts on the screen. The curve is typical of those obtained for other biases.

These data admittedly do not prove that the ions observed with the quadrupole originate in the wind tunnel. Figure 30 does show that a positive ion current does not exist for positive potentials on the entrance hole plate. Additional data are needed before more definite statements can be made.

E. Suggested Future Actions

Mass spectra have been observed and a plausible explanation for positive ion transit through a positive biased entrance hole has been given. Further measurements of the behavior of ions both in the neighborhood of the entrance hole and upstream in the wind tunnel are needed.

Loss of ions between the entrance hole and the quadrupole remains larger than desirable. By shortening the separation between these two points, this loss could probably be reduced.

It is believed that ion spectral measurements can be made and interpreted as characteristic of the ions in the wind tunnel if the work outlined above is completed.

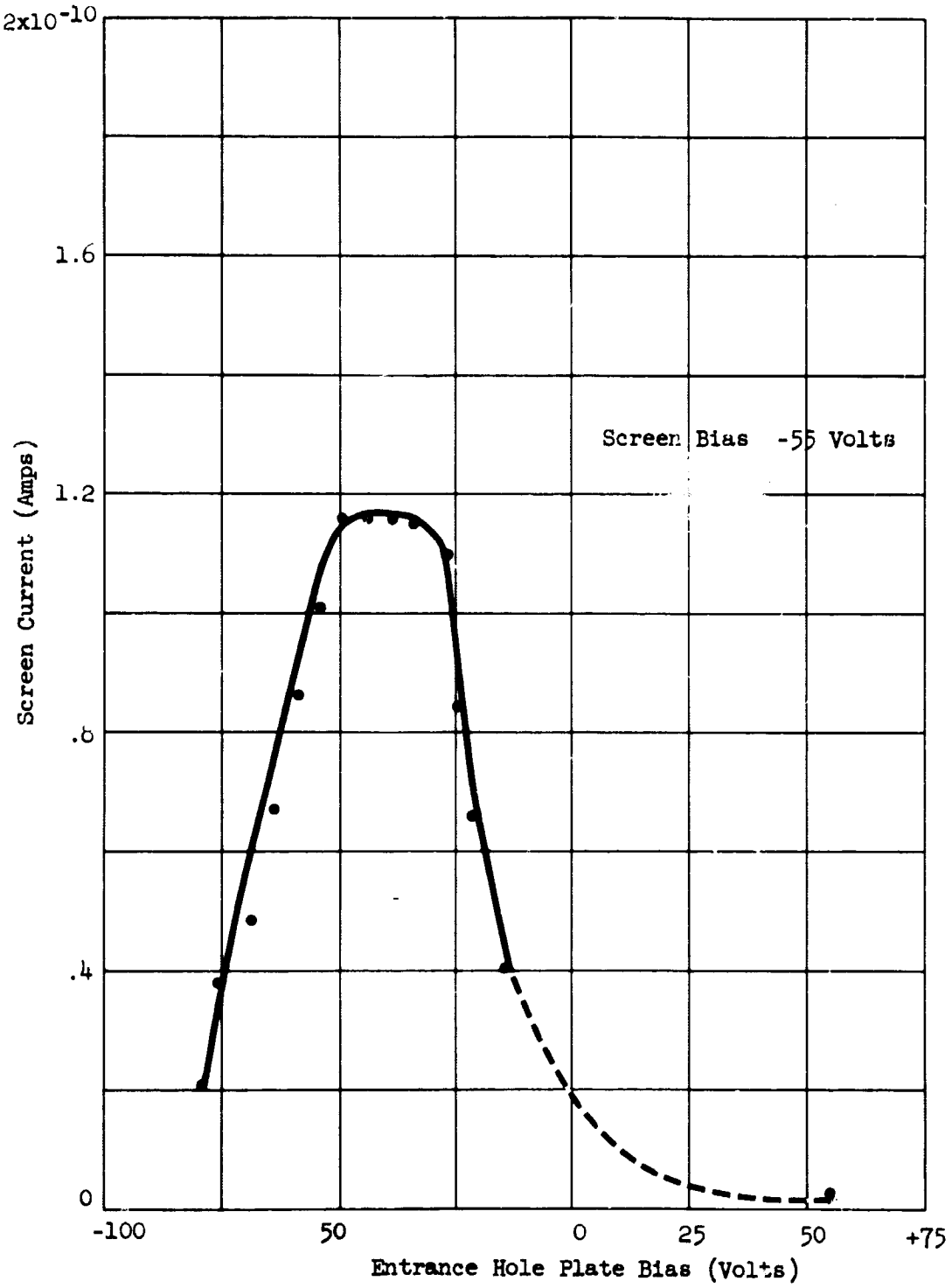

Figure 30

Entrance Hole Transmitted Current

VI. GSFC ION MOBILITY SPECTROMETER

During a two-day visit Mr. P. Serbu and Mr. E. Zelnner of GSFC were able to test their ion mobility spectrometer in the Avco wind tunnel. Observations were made in the 20-35 km altitude range with air flow velocities between 5 and 50 m/sec. The GSFC instrument includes an electronic air flow velocity capability and this feature was used to check pitot tube velocity measurements. Agreement was found to be within 5% at 18 m/sec and as poor as 50% at 5 m/sec.

The sensitivity of the GSFC system was apparently significantly greater than the Avco Gerdien. Mobility spectra were obtained by Serbu and Zelnner using the radioactive source at pressures lower than had been possible with the Avco instrument. It was also found that due to noise or saturation, the corona discharge source could not be used.

In these measurements, the support for the GSFC instrument blocked a large part of the wind tunnel and prevented successful operation of the Quad 150A mass spectrometer.

VII. CONCLUSIONS AND RECOMMENDATIONS

The objective of this contract identified in the introduction of this report was to show by laboratory measurements that a correlation can be made between mobility and mass spectra. It has been reported in the earlier sections that this goal was not quite reached. The principal accomplishments of the contract have been accumulation of mobility spectra at different pressures, the development of a vacuum system which allows the operation of a mass spectrometer within the wind tunnel, and the concurrent measurement of mobility and mass spectra. Certain reservations with respect to ion trajectories in the vicinity of the mass spectrometer vacuum system aperture prevent one from taking the final step of making the necessary correlation between the two kinds of spectra.

To remove these reservations, further experimental work will be required. First, in the area of ion optics, a better method must be found to inject the ions into the quadrupole mass filter. Second, simultaneous mass and mobility spectra for different gas mixtures should be collected to form the basis for the desired correlation.

Nothing has been found in the research which has been carried out in this contract which suggests that the correlation between mobility and ion species will not be proved. It is recommended that the work be continued to this end.

VIII. NEW TECHNOLOGY

Because of the vacuum requirements of a mass spectrometer, an aperture must exist between the higher pressure test region, the wind tunnel in the present work, and the spectrometer. The problem of directing detectable numbers of ions through a small aperture is not trivial and when solved the result will fall within the realm of new technology. The work of this contract has identified this problem area and the recommendations which have been made include its solution. No other new technology has been identified.

IX. REFERENCES

Dolezalek, H. and A. L. Oster, 1965: Spectrometer for Atmospheric Ions in Their Uppermost Range of Mobility (Project: Measuring Ionic Mobilities in the Terrestrial Upper Stratosphere and Mesosphere, Phase I). Final Report Contract DA-19-020-AMC-0058 (X), Avco RAD-TR-65-25, Wilmington, Mass., 4 September 1965, xvi/180 pp.

Gerdien, H., 1905: Demonstration eines Apparates zur absoluten Messung der elektrischen Leitfähigkeit der Luft. Physikalische Zeitschrift, 6, 800-801.

Kahler, K., 1903: Uber die durch Wasserfalle erzeugte Leitfälhigheit der Luft. Ann. d. Physik (4) 12, 1119-1141.

Lenard, P., 1900: Uber die Elektricitatszerstreuung in ultraviolett durchstrahlter Luft. Ann. der Physik (4), 3, 298-319.

Rutherford, E. 1899: Uranium Radiation and the Electrical Conduction Produced by It. Phil. Mag. 47, 109-163.

Zeleny, J., 1900: The Velocity of Ions produced in Gases by Rŏntgen Rays. Phil. Trans. Roy. Soc. London A 195, 193-234.